

Clustering Longitudinal Life-Course Sequences using Mixtures of Exponential-Distance Models

Keefe Murphy^{1,2}, T. Brendan Murphy^{1,2},
 Raffaella Piccarreta³, I. Claire Gormley^{1,2}

¹ School of Mathematics and Statistics, University College Dublin, Ireland

² Insight Centre for Data Analytics, University College Dublin, Ireland

³ Department of Decision Sciences, Università Bocconi, Milan, Italy

E-mail: keefe.murphy@ucd.ie

Abstract

Sequence analysis is an increasingly popular approach for the analysis of life courses represented by an ordered collection of activities experienced by subjects over a given time period. Several criteria exist for measuring pairwise dissimilarities among sequences. Typically, dissimilarity matrices are employed as input to heuristic clustering algorithms, with the aim of identifying the most relevant patterns in the data.

Here, we propose a model-based clustering approach for categorical sequence data. The technique is applied to a survey data set containing information on the career trajectories of a cohort of Northern Irish youths tracked between the ages of 16 and 22.

Specifically, we develop a family of methods for clustering sequences directly, based on mixtures of exponential-distance models, which we call MEDseq. The use of the Hamming distance or weighted variants thereof as the distance metrics permits closed-form expressions for the normalising constant, thereby facilitating the development of an ECM algorithm for model fitting. Additionally, MEDseq models allow the probability of component membership to depend on fixed covariates. Sampling weights, which are often associated with life-course data arising from surveys, are also accommodated. Simultaneously including weights and covariates in the clustering process yields new insights on the Northern Irish data.

Keywords: Life-course data, exponential-distance models, model-based clustering, weighted Hamming distance, gating covariates, survey sampling weights.

1 Introduction

Sequence analysis (SA) is an umbrella term for tools defined to explore and describe categorical life-course data. Specifically, attention is focused on the ordered sequence of states (or activities) experienced by individuals over a given time-span (usually at T equally spaced discrete time periods). The goal of analysis is to identify the most relevant patterns in the data. To this end, pairwise dissimilarities among sequences in their entirety are first assessed. Dissimilarity matrices are then employed to identify the most typical trajectories using, in the vast majority of applications, cluster analysis.

Quantifying the distance between categorical sequences is not a trivial task. Optimal matching (OM), developed by [Abbott and Forrest \(1986\)](#) and extended to sociology by [Abbott and Hrycak \(1990\)](#), is popular among the SA community. OM is derived from the edit distance originally proposed in the field of information theory and computer science by [Levenshtein \(1966\)](#). The OM metric assigns costs to the different types of edits, namely

insertion, deletion, and substitution. Typically, insertion and deletion are assigned a cost of 1 while substitution costs are allowed to vary. However, specifying these costs involves subjective choices, and may lead to violations of the triangle inequality if not done carefully. Several proposals in the literature introduced criteria to improve or guide the choice of costs in OM. Also, alternative dissimilarity criteria have been introduced to allow control over the importance assigned to the characteristics of the sequences (namely, the collection of experienced states, their timing, or their duration) in the assessment of their differences: see [Studer and Ritschard \(2016\)](#) for an excellent discussion. Even so, there are no results proving that one procedure is superior to the others, and the choice of dissimilarity measure remains a fundamental choice left to the researcher.

Given a dissimilarity matrix \mathbf{D} , obtained from a set of sequences $\mathbf{S} = (\mathbf{s}_1, \dots, \mathbf{s}_n)$, where n is the number of subjects, cluster analysis is usually applied to group sequences and to identify the most typical trajectories experienced by the sampled individuals. Typically, heuristic clustering algorithms, either hierarchical or partitional, are used. In many applications, it is also of interest to relate the sequences to a set of baseline covariates. Within the described framework, this is solely done by relating the uncovered clustering partition to covariates, using for example multinomial logistic regression (MLR). This approach is questionable from a few points of view. Firstly, the original sequences are substituted by a categorical variable indicating clustering membership, thus disregarding the heterogeneity within clusters. This is clearly only sensible when the clusters are sufficiently homogeneous. However, a clear clustering structure can often be obtained only by increasing the number of clusters (often with some clusters possibly small in size). More importantly, suitable partitions do not necessarily lead to suitable response variables as input for the MLR. It thus seems desirable to cluster sequences and relate the clusters to the covariates simultaneously.

To address these issues, we propose to cluster trajectories in a model-based fashion, allowing the covariates to guide the construction of the clusters, rather than leaving them exogenous to the clustering model. This permits to better understand if and to what extent specific covariates affect the typical sequence patterns characterising each cluster. Model-based clustering methods typically assume that the data arise from a finite mixture of G distributions; [Bouveyron et al. \(2019\)](#) provide an excellent overview. In principle, any distribution can be used, though the term ‘model-based clustering’ was popularised by [Banfield and Raftery \(1993\)](#), in which the underlying distributions are assumed to be parsimoniously parameterised multivariate Gaussians with component-specific parameters. Such models have been recently extended to the mixture of experts setting ([Gormley and Frühwirth-Schnatter, 2019](#)) to facilitate dependence on fixed covariates ([Murphy and Murphy, 2019](#)). However, these models can be problematic when applied to dissimilarity matrices, either due to non-identifiability or because the input data are usually far from Gaussian. This problem cannot be addressed by applying multidimensional scaling to \mathbf{D} because the resulting low-dimensional configuration is also typically far from Gaussian. Notably, our attempts to fit non-Gaussian mixtures in these settings did not yield useful results.

Another popular framework for clustering categorical data is latent class analysis (LCA; [Lazarsfeld and Henry 1968](#)). [Agresti \(2002\)](#) shows the connection between model-based clustering and LCA. Such models are finite mixtures in which the component distributions are assumed to be multi-way cross-classification tables with all variables mutually independent. Latent class regression models ([Dayton and Macready, 1988](#)) are particularly interesting, because their connection to the mixture of experts framework permits the inclusion of covariates to predict the latent class memberships. However, fitting such models is challenging when the sequence length, the number of categories, or the number of latent classes are even moderately large, due to the explosion in the number of parameters.

For the reasons mentioned above, we model the sequences directly, via parsimonious mixtures of exponential-distance models. Exponential-distance models typically depend on a central sequence and a precision parameter in a way that relates to the chosen distance metric. Mostly for reasons of computational convenience, we use dissimilarities based on simple matching, in particular the Hamming distance (Hamming, 1950). This distance is liable to suffer from temporal rigidity, since anticipations and/or postponements of the same choices in life courses are not accounted for. Hence, similar sequences shifted by one time period may be maximally distant from one another. While misalignment is less of a concern for sequences exhibiting long durations in the same state, we address the issue using weighted variants of the Hamming distance, characterised by a range of constraints on the precision parameters in the mixture setting. This leads to the novel MEDseq family of models, which can be seen as similar to a version of the k -medoids/PAM algorithm (Kaufman and Rousseeuw, 1990) based on the Hamming distance with some restrictions relaxed.

Our approach is illustrated using data from the 1999 sweep of the Status Zero Survey (McVicar, 2000; McVicar and Anyadike-Danes, 2002) – henceforth referred to as the MVAD data – on the school-to-work trajectories experienced by a cohort of Northern Irish youths. McVicar and Anyadike-Danes (2002) apply Ward’s agglomerative hierarchical clustering algorithm to an OM dissimilarity matrix to obtain $G = 5$ clusters of these trajectories, without performing model selection. Thereafter, they use MLR to relate the hard assignments of trajectories to the clusters to a set of baseline covariates. We instead cluster the MVAD data in a model-based fashion, using the MEDseq model family, and allow the covariates to guide the construction of the clusters by assuming they influence the probability of component membership. Importantly, information is also available on the survey sampling weights, which are only incorporated in the MLR stage of the analysis in McVicar and Anyadike-Danes (2002). While sampling weights can be incorporated into heuristic clustering algorithms, such as Ward’s hierarchical clustering (by weighting the linkages between clusters) or k -medoids, and subsequently in the MLR, one of the advantages of our approach is that both the covariates and the weights are incorporated simultaneously.

MEDseq models, like standard SA heuristic clustering algorithms and LCA models, approach the clustering task from the holistic perspective of modelling whole trajectories, in order to uncover groups of similar sequences. In contrast, a number of multistate models employing finite mixtures of Markov components (e.g. Melnykov 2016a; Paminger and Frühwirth-Schnatter 2010) or hidden-Markov components (Helske et al., 2016) have recently attained popularity for the analysis of categorical sequence data. Such models focus on modelling instantaneous transitions within the life course and on factors that might explain the probability of experiencing them. As described by Wu (2000), this amounts to a difference between considering sequences in their entirety under the MEDseq framework or as time-to-event processes under the Markovian framework.

The remainder of the article is organised as follows. Section 2 presents some exploratory analysis of the MVAD data. Section 3 develops the MEDseq family of mixtures of exponential-distance models that account for sampling weights and allow potential dependency on covariates. Section 4 describes the model fitting procedure and discusses factors affecting performance. Section 5 presents results for the MVAD data, including applications of MEDseq models and comparisons to other methods. The insights gleaned from the MVAD data under the optimal MEDseq model are summarised in Section 6. The paper concludes with a brief discussion on the MEDseq methodology and potential future extensions in Section 7. A software implementation for the full MEDseq model family is provided by the associated R package MEDseq (Murphy et al., 2019), which is available from www.r-project.org (R Core Team, 2019), with which all results were obtained.

2 Status Zero Survey: MVAD Data

The term ‘MVAD data’ refers throughout to a cohort of $n = 712$ Northern Irish youths aged 16 and eligible to leave compulsory education as of July 1993 who were observed at monthly intervals until June 1999 as part of the Status Zero Survey (McVicar, 2000; McVicar and Anyadike-Danes, 2002). The subjects were interviewed about the labour market activities they experienced, distinguishing between employment (EM), further education (FE), higher education (HE), joblessness (JL), school (SC), or training (TR). Each observation i is represented by an ordered categorical sequence of length $T = 72$, with an alphabet of $v = 6$ possible categories, e.g. $\mathbf{s}_i = (s_{i,1}, s_{i,2}, \dots, s_{i,72})^\top = (\text{SC}, \text{SC}, \dots, \text{TR}, \text{TR}, \dots, \text{EM}, \text{EM})^\top$. Notably, the transitions HE \rightsquigarrow SC and TR \rightsquigarrow HE are never observed. The sequences share a common length, the time periods are equally spaced, and there are no missing data.

It is of interest to relate the MVAD sequences to covariates in order to understand whether different characteristics – related to gender, community, geographic and social conditions, and personal abilities – impact on the school-to-work trajectories. These covariates are summarised in Table 1. All covariates were measured at the age of 16 (i.e. at the start of the study period in July 1993), with the exception of ‘Funemp’ and ‘Livboth’, and are thus static background characteristics. The MVAD data also come with associated observation-specific survey sampling weights. Each sample was weighted based on the first state value at age 16, and the ‘Grammar’ and ‘Location’ covariates (McVicar and Anyadike-Danes, 2002).

Table 1: Available covariates for the MVAD data set. For binary covariates, the event denoted by 1 is indicated. Otherwise, the levels of the categorical covariate ‘Location’ are grouped in curly brackets.

Covariate	Description
Gender	1=male
Catholic	1=yes
Grammar	Type of secondary education, 1=grammar school
Funemp	Father’s employment status as of June 1999, 1=employed
GCSE5eq	Qualifications gained by the end of compulsory education, 1=5+ GCSEs at grades A-C, or equivalent
FMPR	SOC code of father’s current or most recent job as of the beginning of the survey, 1=SOC1 (professional, managerial, or related)
Livboth	Living arrangements as of June 1995, 1=living with both parents
Location	{Belfast, N. Eastern, Southern, S. Eastern, Western}

The MVAD data are available in the R packages `MEDseq` and `TraMineR` (Gabadinho et al., 2011). As the data have been used to illustrate some of the functionalities of the `TraMineR` package in its associated vignette¹, interesting features of an exploratory analysis of the data can be found therein. However, we reproduce plots of the transversal state distributions in Figure 1 and the transversal Shannon entropies in Figure 2, i.e. the entropies of each time point of the state distribution (Billari, 2001). Note that the sampling weights are accounted for in both cases.

Figure 1 shows that the number of subjects who found employment increased over time. Conversely, fewer students were in training or further education by the end of the observation period. Most students appear to have entirely left school within 2/3 years of the commencement of the survey. Interestingly, many students were jobless during the first two months of observation, possibly because this period coincided with the summer break from school. Finally, while students only began to pursue higher education from July 1995 onwards, a number of students had already pursued further education during the two preceding years. Figure 2 confirms that the heterogeneity of the state distribution varies over time. In particular, the entropies decline after Sep 1995, by which point most students had left school.

¹ cran.r-project.org/web/packages/TraMineR/vignettes/TraMineR-state-sequence.pdf

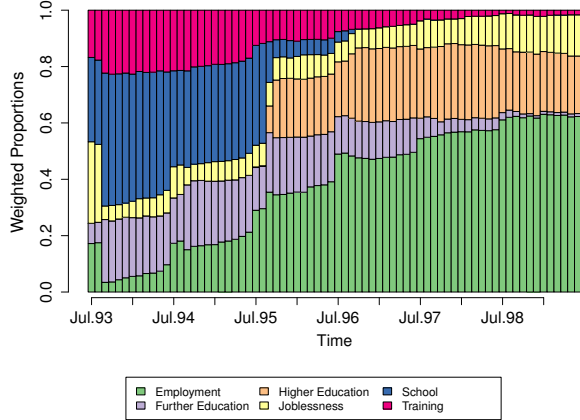


Figure 1: Overall state distribution for the weighted MVAD data.

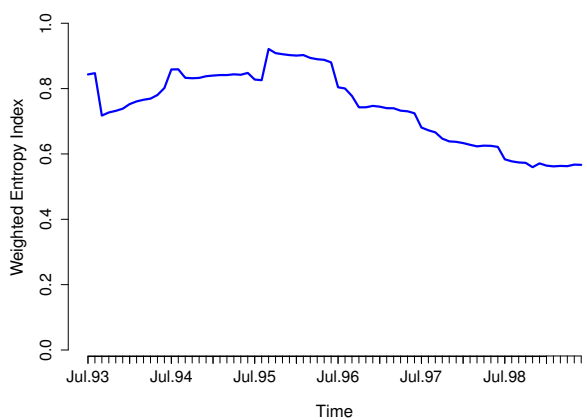


Figure 2: Transversal entropy plot for the weighted MVAD data.

3 Modelling

In this section, we introduce the family of MEDseq models. The exponential-distance model is described in Section 3.1, extended to account for sampling weights in Section 3.2, expanded into a family of mixtures in Section 3.3, and finally embedded within the mixture of experts framework in Section 3.4 in order to accommodate covariates.

3.1 Exponential-Distance Models

For an arbitrary distance metric $d(\cdot, \cdot)$, a location parameter $\boldsymbol{\theta}$, and a precision parameter λ , the probability mass function (PMF) of an exponential-distance model for sequences is

$$f(\mathbf{s}_i | \boldsymbol{\theta}, \lambda, d) = \frac{\exp(-\lambda d(\mathbf{s}_i, \boldsymbol{\theta}))}{\sum_{\mathbf{s}_i \in \mathbf{S}'} \exp(-\lambda d(\mathbf{s}_i, \boldsymbol{\theta}))} = \Psi(\lambda, \boldsymbol{\theta} | T, v)^{-1} \exp(-\lambda d(\mathbf{s}_i, \boldsymbol{\theta})), \quad (1)$$

with the corresponding log-likelihood function given by

$$\ell(\boldsymbol{\theta}, \lambda | \mathbf{S}, d) = \sum_{i=1}^n \log f(\mathbf{s}_i | \boldsymbol{\theta}, \lambda, d) = -\lambda \sum_{i=1}^n d(\mathbf{s}_i, \boldsymbol{\theta}) - n \log \Psi(\lambda, \boldsymbol{\theta} | T, v). \quad (2)$$

Such a model is analogous to the Gaussian distribution (characterised by the squared Euclidean distance from the mean) and similar to the Mallows model for permutations (Mallows, 1957). Indeed, mixtures of Mallows models have been used to cluster rankings (Murphy and Martin, 2003). We only consider models with $\lambda \geq 0$. When $\lambda = 0$, the distribution of sequences is uniform. For $\lambda > 0$, the central sequence $\boldsymbol{\theta}$ is the mode, i.e. the sequence with highest probability, and the probability of any other sequence decays exponentially as its distance from $\boldsymbol{\theta}$ increases. The precision parameter λ controls the speed of this decay. Larger λ values cause sequences to concentrate around $\boldsymbol{\theta}$, tending toward a point-mass as $\lambda \rightarrow \infty$. Notably, λ is not identifiable when all sequences are identical.

The log-likelihood in (2) is generally intractable, as the normalising constant $\Psi(\lambda, \boldsymbol{\theta} | T, v)$ depends on λ (and possibly also on $\boldsymbol{\theta}$, for some more complicated distances), as well as the fixed constants T and v , and requires a sum over all possible sequences. With reference to the MVAD data, for example, the computation of $\Psi(\lambda, \boldsymbol{\theta} | T, v)$ is practically infeasible because there are $v^T = 6^{72}$ possible sequences. Fortunately, however, the normalising constant exists in closed form under the Hamming distance, $d_H(\mathbf{s}_i, \mathbf{s}_j) = \sum_{t=1}^T \mathbb{1}(s_{i,t} \neq s_{j,t})$, in a manner

which facilitates direct enumeration and crucially does not depend on $\boldsymbol{\theta}$. Consider, for example, the Hamming distances between all ternary ($v = 3$) sequences of length $T = 4$. From the arbitrary reference sequence $(0, 0, 0, 0)$, there is 1 instance of a distance of 0, 8 instances of a distance of 1, 24 instances of a distance of 2, 32 instances of a distance of 3, and 16 instances of a distance of 4. Therefore, $\Psi_H(\lambda | T, v) = e^0 + 8e^{-\lambda} + 24e^{-2\lambda} + 32e^{-3\lambda} + 16e^{-4\lambda}$. Hence, the normalising constant under the Hamming distance metric depends on the parameter λ , the sequence length T , and the number of categories v , and simplifies greatly:

$$\Psi_H(\lambda | T, v) = \sum_{p=0}^T \binom{T}{p} (v-1)^p \exp(-\lambda p) = ((v-1)e^{-\lambda} + 1)^T. \quad (3)$$

Inspired by the generalised Mallows model (Irurozki et al., 2019), the model in (1) based on the Hamming distance can be extended to one based on the weighted Hamming distance. By introducing T precision parameters $\lambda_1, \dots, \lambda_T$, one for each time point (i.e. sequence position), and expressing the exponent in (1) as $d_{WH}(\mathbf{s}_i, \boldsymbol{\theta}) = \sum_{t=1}^T \lambda_t \mathbf{1}(s_{i,t} \neq \theta_t)$ rather than $\lambda d_H(\mathbf{s}_i, \boldsymbol{\theta}) = \lambda \sum_{t=1}^T \mathbf{1}(s_{i,t} \neq \theta_t)$, different time periods can contribute differently to the overall distance, weighted according to the period-specific precision parameters. Thus, the distance from a sequence to the central sequence under the weighted Hamming distance becomes a sum of the precision parameters associated with each time point which differs from the corresponding central sequence position. This allows modelling a situation in which there is high consensus regarding the state values of some time period(s), with a large uncertainty about the values of others, and can help to prevent sequences the same distance from $\boldsymbol{\theta}$ from having the same probability. Returning to the MVAD data, the non-constant transversal entropies in Figure 2 suggest that such an extension may be fruitful. The extension requires rewriting the log-likelihood in (2) with the weighted Hamming distance decomposed into its T components and the normalising constant (3) also modified:

$$\ell(\boldsymbol{\theta}, \lambda_1, \dots, \lambda_T | \mathbf{S}, d_{WH}) = - \sum_{i=1}^n \left[\sum_{t=1}^T \left(\lambda_t \mathbf{1}(s_{i,t} \neq \theta_t) + \log((v-1)e^{-\lambda_t} + 1) \right) \right].$$

Though other dissimilarity measures are available for sequences, we henceforth consider only the Hamming or weighted Hamming distances. The Hamming distance in our setting can be seen as a special case of OM with all substitution costs equal to λ and no insertions or deletions. The weighted Hamming distance is similar to the dynamic Hamming distance (Lesnard, 2010), a prominent alternative to OM, in the sense of having time-varying substitution costs. However, the substitution costs in our model are always assumed to be common with respect to each pair of states. Hence, the weighted Hamming distance corresponds to the Gower distance (Gower, 1971) with equally weighted states and equally or unequally weighted time points.

3.2 Incorporating Sampling Weights

Sampling weights are frequently used for life-course data, as the data typically arise from surveys where the weights are used to correct for representativity bias or stratified sampling schemes. Following Chambers and Skinner (2003), the sampling weights $\mathbf{w} = w_1, \dots, w_n$ are incorporated into the exponential-distance model by simply raising every element of the likelihood to the power of the corresponding weight w_i .

A secondary benefit of this extension is that it facilitates computational gains in the presence of duplicate observations. Such duplicates are quite likely when dealing with discrete life-course data. Indeed, non-uniqueness can be exploited using likelihood weights for

computational efficiency, by fitting models to the subset of unique sequences only, weighted by the product of their occurrence frequencies and their sampling weights (if available, otherwise $w_i = 1 \forall i$). The number of duplicates clearly lowers when considering both the sequences themselves and their associated covariate patterns. In particular, all observations are unique when there are continuous covariates. Nonetheless, in many applications – e.g. the MVAD data (see Table 1) – the covariates are all categorical. Hence, exploiting occurrence frequencies in this manner can be extremely convenient. For instance, only 557 of the $n = 712$ sequences in the MVAD data set are distinct.

3.3 A Family of Mixtures of Exponential-Distance Models

Extending the exponential-distance model with the Hamming distance and sampling weights to the model-based clustering setting yields a weighted likelihood function of the form

$$\mathcal{L}^{\mathbf{w}}(\lambda, \boldsymbol{\theta}_1, \dots, \boldsymbol{\theta}_G | \mathbf{S}, \mathbf{w}, d_H) = \prod_{i=1}^n \left[\sum_{g=1}^G \tau_g \frac{\exp(-\lambda d_H(\mathbf{s}_i, \boldsymbol{\theta}_g))}{((v-1)e^{-\lambda} + 1)^T} \right]^{w_i},$$

where the mixing proportions τ_1, \dots, τ_G are positive and sum to 1. Thus, the clustering approach is both model-based and distance-based, thereby bridging the gap between these two ‘cultures’ in the SA community.

The mixture setting naturally suggests a further extension, whereby the precision parameter λ can be constrained or unconstrained across clusters, in addition to the aforementioned possibility for the precision parameters to be constrained or unconstrained across time points. Within a family of models we term ‘MEDseq’, we thus define the CC, UC, CU, and UU models, where the first letter denotes whether precision parameters are constrained (C) or unconstrained (U) across clusters and the second denotes the same across time points. Hence, all but the CC model employ different weighted variants of the Hamming distance.

Given the role played by λ when it takes the value 0, whereby the distribution of the sequences is uniform, it is convenient and natural to include a noise component (denoted by N) whose single precision parameter is fixed to 0. This extension can be added to each of the 4 models above, regardless of how the precision parameters are otherwise specified. This completes the MEDseq model family with the CCN, UCN, CUN, and UUN models. When $G = 1$, the CC, CU, and CCN models can be fitted. When $G = 2$, the CCN and CUN models are equivalent to the UCN and UUN models, respectively, as there is only one non-noise component. As the noise component arises naturally from restricting the parameter space, we consider the noise component as one of the G components, denoted hereafter with the subscript 0. All 8 model types are summarised further in Appendix A.

3.4 Incorporating Covariates

We now illustrate how to incorporate the available covariate information into the clustering process, both to guide the construction of the clusters and to better interpret the type of observation characterising each cluster. As is typical for model-based clustering analyses, the data are augmented in MEDseq models by introducing a latent cluster membership indicator vector $\mathbf{z}_i = (z_{i,1}, \dots, z_{i,G})^\top$, where $z_{i,g} = 1$ if observation i belongs to cluster g and $z_{i,g} = 0$ otherwise. An advantage of the MEDseq approach is that it can be easily extended to incorporate the possible effects of covariates on the sequence trajectories by allowing the covariates to influence the distribution of the latent variable \mathbf{z}_i .

The inclusion of covariates is achieved under the mixture of experts framework (Jacobs et al., 1991; Gormley and Frühwirth-Schnatter, 2019), by extending the mixture model to allow the mixing proportions for observation i to depend on covariates \mathbf{x}_i . This is particularly attractive as the interpretation of the remaining component-specific parameters is the same as it would be under a model without covariates. For example, in the case of the CC MEDseq model

$$f(\mathbf{s}_i | \lambda, \boldsymbol{\theta}_1, \dots, \boldsymbol{\theta}_G, \mathbf{x}_i, w_i, d_H) = \left[\sum_{g=1}^G \tau_g(\mathbf{x}_i) \frac{\exp(-\lambda d_H(\mathbf{s}_i, \boldsymbol{\theta}_g))}{((v-1)e^{-\lambda} + 1)^T} \right]^{w_i},$$

where the mixing proportions $\tau_g(\mathbf{x}_i)$ are referred to as ‘gates’ or the ‘gating network’, with $\tau_g(\mathbf{x}_i) > 0$ and $\sum_{g=1}^G \tau_g(\mathbf{x}_i) = 1$, as usual. Such a model can be seen as a conditional mixture model (Bishop, 2006) because, given the covariates \mathbf{x}_i , the distribution of the sequences is a finite mixture model under which \mathbf{z}_i has a multinomial distribution with a single trial and probabilities equal to $\tau_g(\mathbf{x}_i)$. The distance-based k -medoids algorithm, though closely related (see Section 4.2), does not accommodate the inclusion of covariates.

Incorporating covariates in ‘hard’ clustering algorithms using MLR, as per McVicar and Anyadike-Danes (2002), has been criticised because the hard assignment of extraneous cases can negatively impact internal cluster cohesion and the MLR coefficient estimates (Piccarreta and Studer, 2019). An advantage of the noise component in MEDseq models is that it captures uniformly distributed sequences that deviate from those in the other, more defined clusters. Filtering outliers in this way lessens their impact on the non-noise gating network coefficients, thereby enabling more accurate inference and improving the interpretability of the effects of the covariates. Moreover, the ‘soft’ partition obtained under the model-based paradigm allows the cluster membership probabilities for sequences lying on the boundary between two neighbouring clusters to be quantified and the effect of such sequences on the gating network coefficients to be mitigated.

As per Murphy and Murphy (2019), the CCN, UCN, CUN, and UUN models which include an explicit noise component can be restricted to having covariates only influence the mixing proportions for the non-noise components, with all observations therefore assumed to have equal probability of belonging to the uniform noise component (i.e. by replacing $\tau_0(\mathbf{x}_i)$ with τ_0). We refer to the former setting as the gated noise (GN) model and to the latter as the non-gated noise (NGN) model. Gating covariates can only be included when $G \geq 2$ under the GN model or when there are 2 or more non-noise components under the NGN model.

4 Model Estimation

This section describes the strategy employed for model fitting and some implementation issues that arise in practice. Specifically, Section 4.1 outlines the ECM algorithm employed for parameter estimation, Section 4.2 discusses the initialisation of the ECM algorithm with reference to the similarities between MEDseq models and the k -medoids algorithm, and the issues of model selection and variable selection are treated in Section 4.3.

4.1 Model Fitting via ECM

Parameter estimation is greatly simplified by the existence of a closed-form expression for the normalising constant for MEDseq models under the Hamming or weighted Hamming distances. We focus on maximum likelihood estimation using a simple variant of the EM algorithm (Dempster et al., 1977). For simplicity, model fitting details are described chiefly for the CC MEDseq model with sampling weights and gating covariates. Additional details

for other model types are deferred to Appendix B. The complete data likelihood for the CC model is given by

$$\mathcal{L}_c^{\mathbf{w}}(\lambda, \boldsymbol{\theta}_1, \dots, \boldsymbol{\theta}_G | \mathbf{S}, \mathbf{X}, \mathbf{Z}, \mathbf{w}, d_H) = \prod_{i=1}^n \left[\prod_{g=1}^G \left(\tau_g(\mathbf{x}_i) \frac{\exp(-\lambda d_H(\mathbf{s}_i, \boldsymbol{\theta}_g))}{((v-1)e^{-\lambda} + 1)^T} \right)^{z_{i,g}} \right]^{w_i},$$

and the complete data log-likelihood hence has the form

$$\ell_c^{\mathbf{w}}(\lambda, \boldsymbol{\theta}_1, \dots, \boldsymbol{\theta}_G | \mathbf{S}, \mathbf{X}, \mathbf{Z}, \mathbf{w}, d_H) = \sum_{i=1}^n \sum_{g=1}^G z_{i,g} w_i [\log \tau_g(\mathbf{x}_i) - \lambda d_H(\mathbf{s}_i, \boldsymbol{\theta}_g) - T \log((v-1)e^{-\lambda} + 1)]. \quad (4)$$

Under this model, the distribution of \mathbf{s}_i depends on the latent cluster membership variable \mathbf{z}_i , which in turn depends on covariates \mathbf{x}_i , while \mathbf{s}_i is independent of \mathbf{x}_i conditional on \mathbf{z}_i .

The iterative algorithm for MEDseq models follows in a similar manner to that for standard mixture models. It consists of an E-step (expectation) which replaces for each observation the missing data \mathbf{z}_i with their expected values $\hat{\mathbf{z}}_i$, followed by a M-step (maximisation), which maximises the expected complete data log-likelihood. The M-step is replaced by a series of conditional maximisation (CM-steps) in which each parameter is maximised individually, conditional on the other parameters remaining fixed. Hence, model fitting is in fact conducted using an expectation conditional maximisation (ECM) algorithm (Meng and Rubin, 1993). Aitken's acceleration criterion is used to assess convergence of the non-decreasing sequence of weighted log-likelihood estimates (Böhning et al., 1994). Parameter estimates produced on convergence achieve at least a local maximum of the weighted likelihood function. Upon convergence, cluster memberships are estimated via the maximum *a posteriori* (MAP) classification.

The E-step (with similar expressions when λ is unconstrained across clusters and/or time points) involves computing expression (5), where $(m+1)$ is the current iteration number:

$$\begin{aligned} \hat{z}_{i,g}^{(m+1)} &= \mathbb{E}\left(z_{i,g} \mid \mathbf{s}_i, \mathbf{x}_i, \hat{\boldsymbol{\theta}}_g^{(m)}, \hat{\lambda}^{(m)}, \hat{\boldsymbol{\beta}}_g^{(m)}, w_i, d_H\right) \\ &= \frac{\hat{\tau}_g^{(m)}(\mathbf{x}_i) f(\mathbf{s}_i \mid \hat{\boldsymbol{\theta}}_g^{(m)}, \hat{\lambda}^{(m)}, w_i, d_H)}{\sum_{g=1}^G \hat{\tau}_g^{(m)}(\mathbf{x}_i) f(\mathbf{s}_i \mid \hat{\boldsymbol{\theta}}_g^{(m)}, \hat{\lambda}^{(m)}, w_i, d_H)}. \end{aligned} \quad (5)$$

Note that the weights w_i in the numerator and denominator cancel each other out, leaving the E-step unchanged regardless of the inclusion or exclusion of weights.

Subsequent subsections describe the CM-steps for estimating the remaining parameters in the model. These individual CM-steps rely on the current estimates $\hat{\mathbf{Z}}^{(m+1)} = (\hat{\mathbf{z}}_1^{(m+1)}, \dots, \hat{\mathbf{z}}_n^{(m+1)})$ to provide estimates of the regression coefficients $\hat{\boldsymbol{\beta}}_g^{(m+1)}$, and hence the mixing proportion parameters $\hat{\tau}_g^{(m+1)}(\mathbf{x}_i)$, as well as the central sequence(s) $\hat{\boldsymbol{\theta}}_g^{(m+1)}$ and component precision parameter(s) $\hat{\lambda}^{(m+1)}$. It is clear from (4) that the sampling weights can be accounted for by simply multiplying every $\hat{z}_{i,g}^{(m+1)}$ by the corresponding weight w_i . Conversely, in the CM-steps which follow, corresponding formulas for unweighted MEDseq models can be recovered by replacing $\hat{z}_{i,g}^{(m+1)} w_i$ with $\hat{z}_{i,g}^{(m+1)}$. The sampling weights for the MVAD data sum to ≈ 711.52 , rather than $n = 712$ though the parameter estimates are not affected by multiplying the weights by a constant value. However, to account for the different characteristics of different weighting systems, all relevant subsequent formulas explicitly account for the sum of the weights, with $W = \sum_{i=1}^n w_i$, so as to focus on the relative importance of each case as a representative of cases in the population.

4.1.1 Estimating the Gating Network Coefficients

The portion of (4) corresponding to the gating network, given by $\sum_{i=1}^n \sum_{g=1}^G z_{i,g} w_i \log \tau_g(\mathbf{x}_i)$, is of the same form as a MLR model with weights given by w_i , here written with component 1 as the baseline reference level, for identifiability reasons:

$$\log \frac{\tau_g(\mathbf{x}_i)}{\tau_1(\mathbf{x}_i)} = \log \frac{\Pr(z_{i,g} = 1)}{\Pr(z_{i,1} = 1)} = \tilde{\mathbf{x}}_i \boldsymbol{\beta}_g \quad \forall g \geq 2, \text{ with } \boldsymbol{\beta}_1 = (0, \dots, 0)^\top,$$

where $\tilde{\mathbf{x}}_i = (1, \mathbf{x}_i)$. Thus, methods for fitting such models can be used to maximise the expectation of this term at each iteration to find estimates of the regression parameters in the gating network $\hat{\boldsymbol{\beta}}_g^{(m+1)}$ and hence the mixing proportions via

$$\hat{\tau}_g^{(m+1)}(\mathbf{x}_i) = \frac{\exp(\tilde{\mathbf{x}}_i \hat{\boldsymbol{\beta}}_g^{(m+1)})}{\sum_{g=1}^G \exp(\tilde{\mathbf{x}}_i \hat{\boldsymbol{\beta}}_g^{(m+1)})}.$$

When there are no gating covariates, the mixing proportions are estimated by $\hat{\tau}_g^{(m+1)} = W^{-1} \sum_{i=1}^n \hat{z}_{i,g}^{(m+1)} w_i$, i.e. the weighted mean of the g -th column of the matrix $\hat{\mathbf{Z}}^{(m+1)}$. However, $\boldsymbol{\tau}$ can also be constrained to be equal (i.e. $\tau_g = 1/G \quad \forall g$) across clusters. Thus, situations where $\tau_{i,g} = \tau_g(\mathbf{x}_i)$, $\tau_{i,g} = \tau_g$, or $\tau_{i,g} = 1/G$ are accommodated.

The standard errors of the MLR in the gating network at convergence are not a valid means of assessing the uncertainty of the coefficient estimates as the cluster membership probabilities are estimated rather than fixed and known. Therefore, we adapt the weighted likelihood bootstrap (WLBS) of O'Hagan et al. (2019) to the MEDseq setting. This is easily implemented by multiplying the sampling weights w_i by draws, for each of B samples, from an n -dimensional symmetric uniform Dirichlet distribution. To ensure stable estimation of the standard errors, $B = 1000$ is used here. To ensure rapid convergence, the estimated $\hat{\mathbf{Z}}$ matrix under the optimal model fit to the full data set is used to initialise the ECM algorithm when refitting models to each sample with corresponding new likelihood weights. Finally, the standard errors of the gating network coefficients across the B samples are obtained.

4.1.2 Estimating the Central Sequences

The location parameter $\boldsymbol{\theta}$ is sometimes referred to as the Fréchet mean or the central sequence. The k -medoids/PAM algorithm, which is closely related to the MEDseq models with certain restrictions imposed (see Section 4.2), fixes the estimate of $\hat{\boldsymbol{\theta}}_g$ to be the medoid of cluster g (Kaufman and Rousseeuw, 1990), i.e. the observed sequence with minimum distance from the others currently assigned to the same cluster. This estimation approach is especially quick as the Hamming distance matrix for the observed sequences is pre-computed. Notably, this greedy search strategy may fail to find the optimum solution.

However, it can be shown – for a single unweighted exponential-distance model based on the Hamming distance – that $\hat{\boldsymbol{\theta}}$ is given simply by the modal sequence, which is intuitive when $d_H(\mathbf{s}_i, \mathbf{s}_j)$ is expressed as $T - \sum_{t=1}^T \mathbf{1}(s_{i,t} = s_{j,t})$. Thus, the parameter has a natural interpretation. For more complicated distance metrics, the first-improvement algorithm (Hoos and Stützle, 2004) or a genetic algorithm could be used to estimate $\boldsymbol{\theta}$. Notably, the modal sequence need not be an observed sequence. It is also notable that the Fréchet mean may be non-unique under any of the proposed estimation strategies.

For the $G > 1$ MEDseq setting, under the ECM framework, central sequence position estimates $\hat{\theta}_{g,t}^{(m+1)}$ are given by $\arg \min_{\vartheta} \left(\sum_{i=1}^n \hat{z}_{i,g}^{(m+1)} w_i \mathbf{1}(s_{i,t} \neq \vartheta) \right)$. Since this expression is independent of the precision parameter(s), it holds for all MEDseq model types, including

those which employ the weighted Hamming distance variants. Thus, $\widehat{\boldsymbol{\theta}}_g$ is estimated easily and exactly via a type of weighted mode, which is composed, for each position in the sequence, by the category corresponding to the maximum of the sum of the weights $\widehat{z}_{i,g}^{(m+1)} w_i$ associated with each of the v observed state values. Similarly, the central sequence under a weighted $G = 1$ model is also estimated via a weighted mode, with the weights given only by w_i . Notably, to estimate the Fréchet mean for a MEDseq model of any type without sampling weights, one need only remove w_i from these terms. Note also that $\boldsymbol{\theta}_0$ does not need to be estimated for the models with an explicit noise component as it does not contribute to the likelihood.

4.1.3 Estimating the Precision Parameters

It is worth noting, for the exponential-distance model in general, with any distance metric, that the method of moments estimate for λ is equal to the maximum likelihood estimate (MLE). This is because, for fixed $\boldsymbol{\theta}$, the PMF in (1) belongs to the exponential family with natural parameter λ . Hence, with $\widehat{\boldsymbol{\theta}}$ already estimated as per Section 4.1.2, $\widehat{\lambda}$ ensures that the expected distance of observations from $\widehat{\boldsymbol{\theta}}$ is equal to the observed average distance from $\widehat{\boldsymbol{\theta}}$, since the solution of

$$\frac{\partial \ell(\lambda | \mathbf{S}, \widehat{\boldsymbol{\theta}}, d)}{n \partial \lambda} = \frac{\sum_{\mathbf{s}_i \in \mathbf{S}'} d(\mathbf{s}_i, \widehat{\boldsymbol{\theta}}) \exp(-\lambda d(\mathbf{s}_i, \widehat{\boldsymbol{\theta}}))}{\sum_{\mathbf{s}_i \in \mathbf{S}'} \exp(-\lambda d(\mathbf{s}_i, \widehat{\boldsymbol{\theta}}))} - \frac{1}{n} \sum_{i=1}^n d(\mathbf{s}_i, \widehat{\boldsymbol{\theta}}).$$

implies

$$\mathbb{E}_\lambda(d(\mathbf{S}, \widehat{\boldsymbol{\theta}})) = \frac{\sum_{\mathbf{s}_i \in \mathbf{S}'} d(\mathbf{s}_i, \widehat{\boldsymbol{\theta}}) \exp(-\lambda d(\mathbf{s}_i, \widehat{\boldsymbol{\theta}}))}{\sum_{\mathbf{s}_i \in \mathbf{S}'} \exp(-\lambda d(\mathbf{s}_i, \widehat{\boldsymbol{\theta}}))} = \bar{d}(\mathbf{S}, \widehat{\boldsymbol{\theta}}) = \frac{1}{n} \sum_{i=1}^n d(\mathbf{s}_i, \widehat{\boldsymbol{\theta}}). \quad (6)$$

Under the Hamming distance, the value of the expectation in (6) holds for any arbitrary reference sequence in place of $\widehat{\boldsymbol{\theta}}$. Hence, with known $\widehat{\boldsymbol{\theta}}$, the MLE for λ for an unweighted single-component CC model can be obtained as follows:

$$\begin{aligned} \ell(\lambda | \mathbf{S}, \widehat{\boldsymbol{\theta}}, d_H) &= -\lambda n \bar{d}_H(\mathbf{S}, \widehat{\boldsymbol{\theta}}) - nT \log((v-1) e^{-\lambda} + 1), \\ \frac{\partial \ell(\cdot)}{\partial \lambda} &= \frac{nT(v-1)}{e^\lambda + (v-1)} - n \bar{d}_H(\mathbf{S}, \widehat{\boldsymbol{\theta}}), \\ \therefore \widehat{\lambda} &= \log \left((v-1) \left(\frac{T}{\bar{d}_H(\mathbf{S}, \widehat{\boldsymbol{\theta}})} - 1 \right) \right). \end{aligned}$$

However, this can yield a negative value for $\widehat{\lambda}$. Recall that we only consider $\lambda \geq 0$. Since all distances are non-negative and typically not identical, $\frac{\partial \ell(\cdot)}{\partial \lambda}$ is negative $\forall \lambda > 0$ in the case where the sufficient statistic $\bar{d}_H(\mathbf{S}, \widehat{\boldsymbol{\theta}}) > v^{-1}T(v-1)$, with $\lim_{\lambda \rightarrow \infty} \frac{\partial \ell(\cdot)}{\partial \lambda} = -n \bar{d}_H(\mathbf{S}, \widehat{\boldsymbol{\theta}})$. Thus,

$$\widehat{\lambda} = \max \left(0, \log \left((v-1) \left(\frac{T}{\bar{d}_H(\mathbf{S}, \widehat{\boldsymbol{\theta}})} - 1 \right) \right) \right).$$

When $\bar{d}_H(\mathbf{S}, \widehat{\boldsymbol{\theta}}) < v^{-1}T(v-1)$, such that $\widehat{\lambda} > 0$, the identity $\log(c(a/b - 1)) = \log(c) + \log(a - b) - \log(b)$ is used for numerical stability, otherwise $\widehat{\lambda}$ is set to 0. When sampling weights are included, following the same steps as above yields the corresponding estimate

$$\widehat{\lambda} = \max \left(0, \log(v-1) + \log \left(\frac{TW}{\sum_{i=1}^n w_i d_H(\mathbf{s}_i, \widehat{\boldsymbol{\theta}})} - 1 \right) \right). \quad (7)$$

While $\widehat{\lambda}$ can potentially be estimated as zero, the inclusion of a noise component in the CCN, UCN, CUN, and UUN models makes this explicit, by restricting one of the clusters to have $\widehat{\lambda}_{g,t} = 0 \forall t = 1, \dots, T$. When $\widehat{\lambda}_{g,t}$ is either estimated as zero or set to zero, estimating the corresponding $\boldsymbol{\theta}_{g,t}$ parameter has no effect on the likelihood.

The ECM algorithm is employed when $G > 1$, in which case the CM-step for $\widehat{\lambda}^{(m+1)}$ under a CC MEDseq mixture model with sampling weights is given by

$$\begin{aligned} \frac{\partial \ell_c^w(\cdot)}{\partial \lambda} &= \frac{T(v-1) \sum_{i=1}^n \sum_{g=1}^G z_{i,g} w_i}{e^\lambda + (v-1)} - \sum_{i=1}^n \sum_{g=1}^G z_{i,g} w_i d_H(\mathbf{s}_i, \widehat{\boldsymbol{\theta}}_g), \\ \therefore \widehat{\lambda}^{(m+1)} &= \max \left(0, \log(v-1) + \log \left(\frac{T \sum_{i=1}^n \sum_{g=1}^G \widehat{z}_{i,g}^{(m+1)} w_i}{\sum_{i=1}^n \sum_{g=1}^G \widehat{z}_{i,g}^{(m+1)} w_i d_H(\mathbf{s}_i, \widehat{\boldsymbol{\theta}}_g^{(m+1)})} - 1 \right) \right). \end{aligned} \quad (8)$$

As per (7), this requires the current estimate of each component's central sequence. Again, as each case has $w_i = 1$ when there are no sampling weights, one need only drop the w_i and W terms from (7) and (8) to estimate the precision parameters of unweighted MEDseq models. The expressions for the weighted complete data likelihoods and corresponding CM-steps for their precision parameters are given for the remaining MEDseq model types in Appendix B.

4.2 ECM Initialisation

The MEDseq models share relevant features with the k -medoids/PAM algorithm based on the Hamming distance. Indeed, MEDseq models differ from PAM only in that i) $\boldsymbol{\theta}_g$ is estimated by the modal sequence rather than the medoid, ii) $\boldsymbol{\tau}$ is estimated, or even dependent on covariates via $\tau_g(\mathbf{x}_i)$, rather than constrained to be equal, iii) λ is allowed to vary across clusters and/or time points, iv) a noise component can be included, and v) the ECM algorithm rather than the classification EM algorithm (CEM; [Celeux and Govaert, 1992](#)) is used. The C-step of the CEM algorithm employed by PAM uses deterministic assignments $\widehat{z}_{i,g}^{(m+1)} = \arg \max_g (\widehat{z}_{i,g}^{(m+1)})$, for which the denominator in (5) need not be evaluated.

In other words, it can be shown that a CC model fitted by CEM (albeit with conditional maximisation steps), with equal mixing proportions and the central sequences estimated by the medoid rather than the modal sequence, is equivalent to k -medoids based on the Hamming distance. Therefore, we apply the k -medoids algorithm to the Hamming distance matrix to initialise the ECM algorithm by obtaining 'hard' starting values for the allocation matrix \mathbf{Z} . In particular, we rely on a weighted version of PAM available in the R package `WeightedCluster` ([Studer, 2013](#)). This strategy is less computationally onerous than using multiple random starts and in our experience also achieves better results than using Ward's hierarchical clustering to inform starting values. For models with an explicit noise component, it is necessary to supply an initial guess of the prior probability τ_0 that observations are noise, and initialise allocations, assuming the last component is the one associated with $\lambda_g = 0$, by multiplying the initial \mathbf{Z} matrix by $1 - \tau_0$ and appending a column in which each entry is τ_0 . We caution that the initial τ_0 should not be too large.

4.3 Model Selection

In the MEDseq setting, the notion of model selection refers to identifying the optimal number of components G in the mixture and finding the best MEDseq model type in terms of constraints on the precision parameters. Variable selection on the subset of covariates included in the gating network can also improve the fit. For a given set of covariates, one

would typically evaluate all model types over a range of G values and choose simultaneously both the model type and G value according to some criterion. Thereafter, different fits with different covariates can be compared according to the same criterion.

The Bayesian Information Criterion (BIC; [Schwarz 1978](#)) includes a penalty term which depends on the number of free parameters. Notably, the penalty term in our setting uses $\log(W)$ rather than $\log(N)$. Preliminary analyses (e.g. Section 5.1) suggest that this penalty term is not strict enough. Indeed, approaches relying on parameter counts may not be fruitful in general for categorical sequence data, although this may simply be an artefact of the weighted Hamming distance metrics employed. Nevertheless, the number of free parameters in the BIC penalty term under each MEDseq model type is summarised in Appendix A.

We turn to silhouette analysis approaches to assess the quality of the clustering in terms of internal cluster cohesion, where high cohesion indicates high between-group distances and strong within-group homogeneity. Typically the silhouette width is defined for clustering methods which produce a ‘hard’ partition ([Rousseeuw, 1987](#)), and the average silhouette width (ASW) or weighted average silhouette width (wASW; [Studer 2013](#)) is used as a model selection criterion. However, [Menardi \(2011\)](#) introduces the density-based silhouette (DBS) for model-based clustering methods. This allows the ‘soft’ assignment information to be used, which would be discarded when using the MAP assignments in the computation of the wASW. The empirical DBS for observation i is given by

$$\widehat{dbs}_i = \frac{\log\left(\frac{\widehat{z}_i^0}{\widehat{z}_i^1}\right)}{\max_{h=1,\dots,n} \left| \log\left(\frac{\widehat{z}_h^0}{\widehat{z}_h^1}\right) \right|}. \quad (9)$$

As observations are assigned to clusters based on the MAP classification, \widehat{dbs}_i is proportional to the log-ratio of the posterior probability associated with the MAP assignment of observation i (denoted by \widehat{z}_i^0) to the maximum posterior probability that the observation belongs to another cluster (denoted by \widehat{z}_i^1). Use of the MAP classification implies $0 \leq \widehat{dbs}_i \leq 1 \forall i$, with high values indicating a well-clustered data point. Ultimately, the mean or the median \widehat{dbs} value can be used both as a global quality measure and as a model selection criterion.

We employ a version of this criterion which is modified in two ways, both to identify optimal models and as a means of validating the chosen model. Firstly, we identify a set of crisply assigned observations having \widehat{z}_i^1 lower than a tolerance parameter ϵ , here set equal to 10^{-100} . These observations are given \widehat{dbs}_i values of 1 and are excluded from the computation of the maximum in the denominator of (9) for reasons of numerical stability. Secondly, we account for the sampling weights by computing a weighted mean density-based silhouette criterion (wDBS). However, neither the wDBS nor wASW criteria are defined for $G = 1$.

Greedy stepwise selection can be used to further refine the models, in terms of guiding the inclusion/exclusion of gating covariates. We propose a bi-directional search strategy in which each step can potentially consist of adding or removing a covariate or adding or removing a non-noise component. Every potential action is evaluated over all possible model types at each step, rather than considering changing the model type as an action in itself. Changing the gating covariates or changing the number of components can affect the model type, as observed by [Murphy and Murphy \(2019\)](#). While this makes the stepwise search more computationally intensive, it is less likely to miss optimal models as it explores the model space. For steps involving both gating covariates and a noise component, models with both the GN and NGN settings can be evaluated and potentially selected.

A backward stepwise search starts from the model including all covariates considered optimal in terms of the number of components G and of the MEDseq model type. On the other hand, a forward stepwise search uses the optimal model with no covariates included as its starting point. In both cases, the algorithm accepts the action yielding the highest increase in the wDBS criterion at each step. The computational benefits of upweighting unique cases and discarding redundant cases are stronger for the forward search, as early steps with fewer covariates are likely to have fewer unique cases across sequence patterns and covariates.

5 Analysing the MVAD Data

Results of fitting MEDseq models to the MVAD data are provided in Section 5.1. All results were obtained via the associated R package `MEDseq` (Murphy et al., 2019). A comparison against other approaches, including hierarchical, partitional, and model-based clustering methods, is included in Section 5.2. A discussion of the insights gleaned from the solution obtained by the optimal MEDseq model is deferred to Section 6.

Due to the weighting scheme used by McVicar and Anyadike-Danes (2002), all results are obtained on a version of the data with the first time point removed. Similarly, the term ‘all covariates’ henceforth refers to all covariates in Table 1 except ‘Grammar’ and ‘Location’. While Murphy and Murphy (2019) show that the same covariate can affect more than one part of a mixture of experts model, and in different ways, removing the quantities used to define the weights eases the interpretability of the results.

5.1 Application of MEDseq

Weighted MEDseq models are fit across a range of G values, across all 8 model types, with all covariates included in the gating network. The noise components, where applicable, are treated using the GN setting. Figure 3 shows the behaviour of the BIC for these models. Similar behaviour is observed for the ICL criterion (Biernacki et al., 2000). Evidently the penalty terms based on parameter counts for these criteria are not large enough. Values of both criteria do not start to decrease until the number of components is very large and models with too many poorly populated components are identified. Thus, both are deemed inadequate as a means of selecting optimal MEDseq models. The k -fold cross-validated likelihood, a model selection criterion which is free from parameter-counting (Smyth, 2000), also penalises insufficiently (with $k = 10$ folds). The Normalised Entropy Criterion (Celeux and Soromenho, 1996), on the other hand, identifies a model with too few components ($G = 2$).

However, using the wDBS criterion (see Figure 4), and again discarding solutions with too few components, a reasonable $G = 10$ UCN model is identified as optimal. Thus, the performance of the wDBS criterion in this setting is found to be superior to the various criteria described above. The same model type and number of components are identified as optimal according to the wDBS criterion when the noise components are treated with the NGN setting, and when the same analysis is repeated with no gating covariates at all. Notably, the wDBS criterion yields the same optimal model in both the GN and NGN settings, and the setting with covariates excluded entirely, regardless of whether the weighted mean or the weighted median of the individual \widehat{dbs} values is used. Interestingly, $G = 10$ appears to roughly coincide with where the plot of BIC values in Figure 3 begins to plateau.

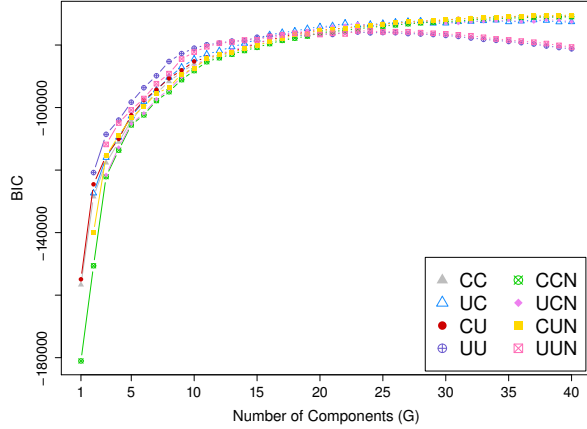


Figure 3: BIC values for weighted MEDseq models across a range of G values and model types.

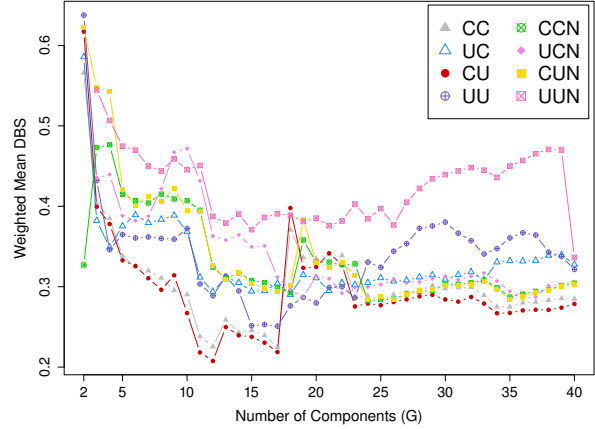


Figure 4: wDBS values for weighted MEDseq models across a range of G values and model types.

In refining the model further via greedy stepwise selection, both the forward search (see Table 2) and backward search (see Table 3) begin with the same number of components and the same model type. Covariates used to define the sampling weights are excluded in both cases. Both searches converge to the same $G = 10$ UCN model with the covariates ‘FMPR’, ‘GCSE5eq’, and ‘Livboth’ in the GN gating network. Under this model, the probability of belonging to the noise component also depends on the included covariates. Notably, the differences between the respective clusterings produced by the models including no covariates, all covariates, and the subset of covariates obtained by stepwise selection are marginal. This can be seen by computing the inner products between all pairs of $\hat{\mathbf{Z}}$ matrices at convergence. For all three pairwise comparisons, the result, when normalised by its row sums, differs only slightly from the 10-dimensional identity matrix. However, the model uncovered by stepwise selection yields both the highest wDBS value and highest BIC value.

Table 2: Summary of the steps taken to improve the wDBS criterion in the forward direction.

Optimal Step	G	Model Type	Gating Covariates	Gating Type	Mean DBS
–	10	UCN	–	–	0.4699
Add ‘GCSE5eq’	10	UCN	GCSE5eq	GN	0.4724
Add ‘Livboth’	10	UCN	FMPR, Livboth	NGN	0.4731
Add ‘FMPR’	10	UCN	FMPR, GCSE5eq, Livboth	GN	0.4745
Stop	10	UCN	FMPR, GCSE5eq, Livboth	GN	0.4745

Table 3: Summary of the steps taken to improve the wDBS criterion in the backward direction.

Optimal Step	G	Model Type	Gating Covariates	Gating Type	Mean DBS
–	10	UCN	Catholic, FMPR, Funemp, GCSE5eq, Gender, Livboth,	GN	0.4717
Remove ‘Catholic’	10	UCN	FMPR, Funemp, GCSE5eq, Gender, Livboth,	GN	0.4735
Remove ‘Funemp’	10	UCN	FMPR, GCSE5eq, Gender, Livboth	GN	0.4740
Remove ‘Gender’	10	UCN	FMPR, GCSE5eq, Livboth	GN	0.4745
Stop	10	UCN	FMPR, GCSE5eq, Livboth	GN	0.4745

These results are not sensitive to the dropping of the first time point or the covariates used to define the sampling weights. Repeating the analysis above with these quantities retained leads to identical inference on the number of components, the MEDseq model type, and the gating covariates identified via stepwise selection. When repeating the analysis with

the sampling weights discarded entirely, the results differ only in that ‘Funemp’ is identified by stepwise selection rather than ‘FMPR’. Finally, in order to ascertain the robustness of the results to a coarsening of the sequences, the analysis was repeated once more with the data taken at six-monthly intervals. Again, identical inference was obtained. Computationally, the ECM algorithm’s runtime was not greatly improved in doing so. Indeed, the MEDseq method scales more poorly with n rather than T (and also v), as the number of weighted likelihood evaluations for large data sets is more computationally expensive than the number of simple distance evaluations required for long sequences.

5.2 Other Clustering Methods

To contrast the MEDseq results with those obtained by other methods, MEDseq models with no covariates and all covariates are compared, in Figure 5, against weighted versions of k -medoids, using the R package `WeightedCluster` (Studer, 2013), and Ward’s hierarchical clustering, both based on the Hamming distance. Finite mixtures with first-order Markov components, fit via the R package `ClickClust` (Melnikov, 2016b), are also included in the comparison. LCA and latent class regression, fit via the R package `poLCA` (Linzer and Lewis, 2011), are not included, as they encounter computational difficulties due to the explosion in the number of parameters even for $G = 3$. As ‘soft’ cluster assignment probabilities are not available for k -medoids or Ward’s hierarchical clustering, their wDBS values cannot be compared. Thus, Figure 5 illustrates a comparison of the wASW values using the MAP classifications where necessary; in so doing, the soft clustering information is discarded.

The `ClickClust` package allows the initial state probabilities to be either estimated or equal to $1/v$ for all categories; both scenarios were considered. Other function arguments were set to their default values. Only the MEDseq models accommodate gating covariates, while all models except the `ClickClust` models accommodate the sampling weights. In all cases, the first time point was dropped. Only the MEDseq model type with the highest wASW for each G value is shown, for clarity. The wASW values for the `ClickClust` models are not shown; they are approximately 0.11 for $G \geq 2$, and negative thereafter. Across all G values, one of the MEDseq model types always outperforms its competitors.

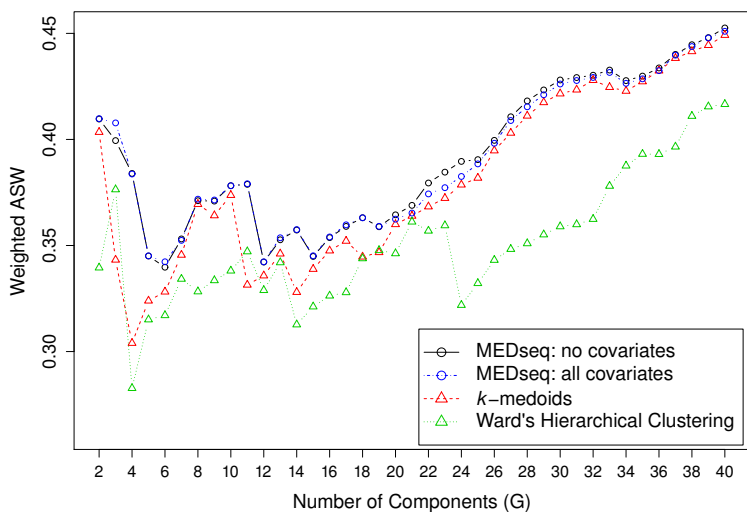


Figure 5: Values of the wASW criterion, using Hamming distances, for the best MEDseq model type for each G value with no covariates and all covariates. Corresponding values for weighted k -medoids and weighted Ward’s hierarchical clustering are also shown.

While the wASW values for the **ClickClust** models being close to zero or even negative shows inferior clustering behaviour, this method also returns a $\widehat{\mathbf{Z}}$ matrix of cluster membership probabilities. Thus, these models can be compared to the MEDseq models in terms of the wDBS criterion also. This is shown in Figure 6. Again, only the best model of each type is shown for each G value. The MEDseq models again exhibit the best performance across the entire range of G values. Notably, the optimal **ClickClust** model according to BIC has only $G = 2$ components. An advantage of **ClickClust** is that it allows sequences of unequal lengths, but this is not a concern for the MVAD data.

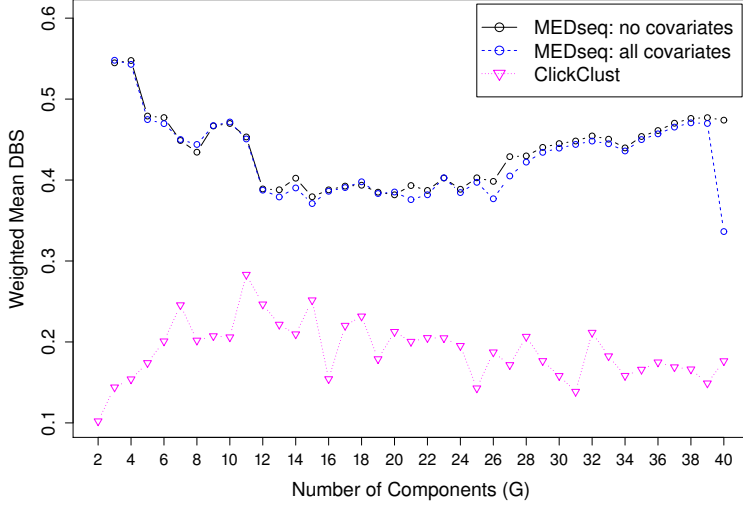


Figure 6: Values of the wDBS criterion for the best MEDseq model type at each G value with no covariates and all covariates. Corresponding values for the best **ClickClust** model are also shown.

The R package **seqHMM** (Helske and Helske, 2019) provides tools for fitting mixtures of hidden Markov models, with gating covariates influencing cluster membership probabilities. However, the sampling weights are not accommodated. Such models allow cluster memberships to evolve over time, similar to mixed membership models (Airoldi et al., 2014). They thus cannot be directly compared to MEDseq models. However, we note that the **seqHMM** package provides a pre-fitted model for the MVAD data with 2 clusters – with 3 and 4 hidden states, respectively – and no covariates. Replicating the same model with the first time point omitted and otherwise using the same function arguments yields a model with wDBS=0.50 and wASW=0.23. Otherwise identical **seqHMM** models, including either all covariates or only those deemed optimal for the MEDseq model using stepwise selection, both achieve wDBS=0.47 and wASW=0.23. Notably, these wDBS values are comparable (albeit inferior) to those for MEDseq models with $G = 2$, while the wASW values are much worse.

6 Discussion of the MVAD Results

The clusters uncovered by the $G = 10$ UCN model deemed optimal according to the wDBS criterion for the MVAD data are shown in Figure 7. Seriation has been applied using the overall Hamming distance matrix (Hahsler et al., 2008) to group observations within clusters for visual clarity. To better inform a discussion of these results, corresponding central sequence estimates are shown in Figure 8 and the average time spent in each state by cluster – weighted by the estimated cluster membership probabilities – is shown in Table 4, along with the cluster sizes.

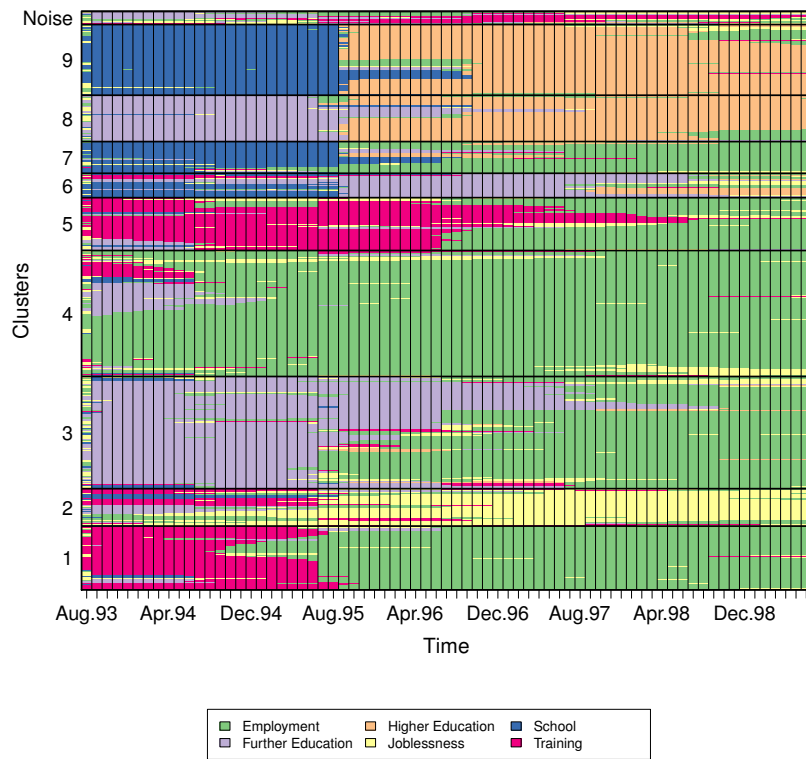


Figure 7: Clusters uncovered using the wDBS criterion for the optimal 10-component UCN model with stepwise selection of covariates.

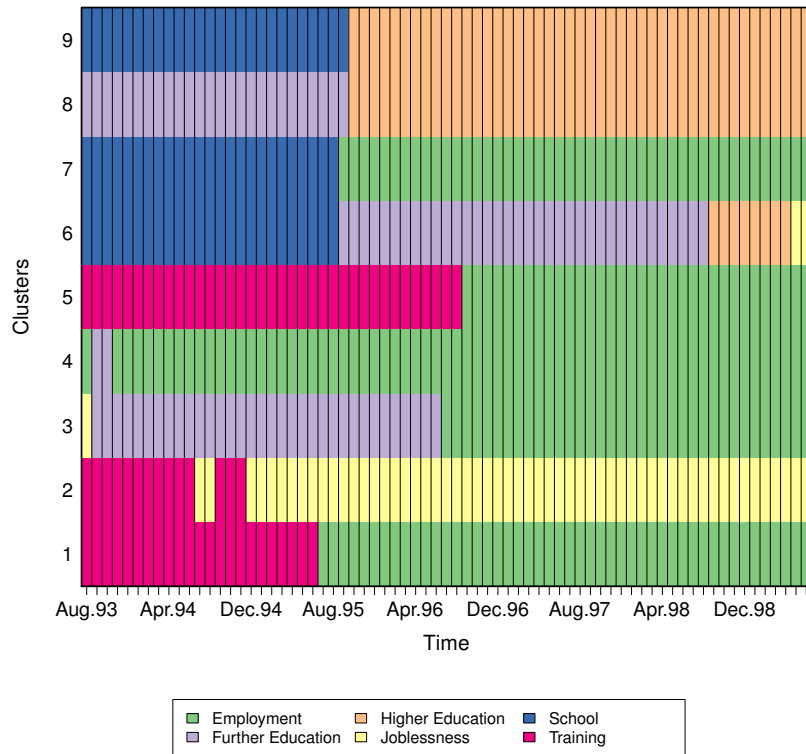


Figure 8: Central sequences of the optimal 10-component UCN model with stepwise selection of covariates. The noise component's central sequence is not shown, as it does not contribute to the likelihood.

Table 4: Average time (in months) spent in each state by cluster, weighted by the estimated cluster membership probabilities, for the optimal 10-component UCN model with stepwise selection of covariates. Estimated cluster sizes \hat{n}_g correspond to the MAP partition.

Cluster (g)	\hat{n}_g	EM	FE	HE	JL	SC	TR
1	79	47.79	1.79	0.00	2.29	0.50	18.63
2	46	9.67	4.38	0.00	43.96	2.76	10.23
3	138	33.66	30.96	1.16	3.31	0.73	1.18
4	155	61.83	2.99	0.00	3.55	0.48	2.15
5	65	28.25	2.84	0.00	5.11	0.89	33.91
6	30	6.42	33.27	7.40	4.23	16.36	3.32
7	39	37.68	2.81	2.59	2.68	23.73	1.52
8	57	4.46	27.19	37.79	0.77	0.79	0.00
9	87	4.44	0.50	38.00	1.35	26.41	0.30
Noise	16	14.15	17.66	1.97	14.39	2.37	20.46

This solution tends to group individuals who experienced trajectories that are similar or that differ only for relatively short periods. In particular, the dominating combinations of states experienced over time are clearly identified, and differences in durations and/or age at transition are quite limited in size. Within clusters, substantial reduction of misalignments and/or differences in the durations of states are evident. Ultimately the partition is characterised not only by the sequencing (i.e. the experienced combinations of states), but also by the durations of the states and by the ages at transitions which appear mostly homogeneous within clusters. This can be explained by the fact that cases in the identified groups tended to dedicate the same period of time – 1, 2, or 3 years – to further/higher education and/or training. This is interesting because one might expect the chosen dissimilarity metric to attach higher importance to the sequencing.

The 10-cluster solution for the MVAD data separates individuals who prolonged their studies after the end of compulsory education (clusters 3, 6, 7, 8, and 9) from those who entered the labour market (clusters 1, 4, and 5). Interestingly, individuals who experienced prolonged periods of unemployment are mostly isolated in cluster 2; this is particularly important because the Status Zero Survey originally aimed to identify such ‘at risk’ subjects.

Notably, the optimal model identified is a UCN model, i.e. one whose precision parameters vary only across clusters, and not across time points. The estimated precision parameters, given in Table 5, show that the model captures different degrees of homogeneity in the cluster-specific sequence distributions. The sequences in clusters 1, 8, and 9, for instance, show greater heterogeneity than the more uniformly distributed sequences in clusters 2, 3, and 6. Thus, model selection favours a model based on the simple Hamming distance (albeit weighted differently in each cluster) rather than a more flexible variant which allows different time periods to contribute differently to the overall distance via period-specific weights. Note that the wDBS criterion used to identify the model is not based on parameter counts, meaning the UCN model is not chosen over a more flexible alternative on the basis of parsimony.

Table 5: Precision parameters of the optimal 10-component UCN model with stepwise selection of covariates. By definition, $\lambda_g = 0$ characterises the noise component.

Cluster (g)	1	2	3	4	5	6	7	8	9	Noise
$\hat{\lambda}_g$	3.81	2.22	2.77	3.11	2.84	2.45	3.08	3.49	3.63	0

Clusters 6, 7 and 9 include subjects who continued school for about two years, presumably to retake previously failed examinations or to pursue academic or vocational qualifications. These individuals are split into three groups depending on whether they continued their studies (further education – cluster 6, or higher education – cluster 9) or were employed directly (cluster 7). Clusters 3 and 8 group subjects who entered further education,

for about two years (or more, in some cases in the larger cluster 3). Most of the subjects in cluster 3 entered employment directly after further education, whereas the vast majority of those in cluster 8 continued in further education until the end of the observation period.

As for the clusters of individuals who moved quickly to the labour market after the end of compulsory education, it is possible to distinguish between individuals who immediately found a job and remained in employment for most of the observation period (the large cluster 4) and individuals who entered government-supported training schemes (clusters 1 and 5). A further separation is between subjects who were employed after about 2 years of training (cluster 1) and those who participated in training for a much longer period (cluster 5). Importantly, most of the individuals in these two clusters were able to find a job even if some respondents experienced some periods of unemployment.

It is interesting to observe that the cluster of careers dominated by persistent unemployment (cluster 2) is characterized by different experiences at the end of the compulsory education period. Indeed, some subjects entered employment directly after the end of compulsory education but left or lost their job after some months, while some prolonged their education before becoming unemployed. However, the majority entered a training period that did not evolve into steady employment.

The coefficients of the gating network with associated WLBS standard errors are given in Table 6, from which a number of interesting effects can be identified. The interpretation of the effects of the covariates is made clearer by virtue of the lower number included after stepwise selection. For completeness, gating network coefficients and associated WLBS standard errors for the model with all covariates included are provided in Appendix C.

Table 6: Multinomial logistic regression coefficients and associated WLBS standard errors (in parentheses) for the gating network of the optimal 10-component UCN model with stepwise selection of covariates.

Cluster	(Intercept)	FMPR	GCSE5eq	Livboth
2	-0.46 (0.45)	-0.54 (0.56)	-0.22 (0.70)	0.08 (0.51)
3	0.04 (0.39)	0.29 (0.45)	1.30 (0.46)	-0.30 (0.42)
4	0.48 (0.38)	-0.89 (0.44)	-0.25 (0.53)	-0.21 (0.37)
5	-0.16 (0.43)	-0.27 (0.52)	0.17 (0.59)	-0.07 (0.43)
6	-2.38 (0.91)	0.62 (0.63)	2.03 (0.75)	1.43 (0.72)
7	-0.19 (0.49)	-0.66 (0.57)	1.37 (0.59)	-0.03 (0.51)
8	-3.21 (0.50)	0.28 (0.47)	3.34 (0.55)	1.12 (0.49)
9	-1.76 (0.49)	0.71 (0.43)	3.85 (0.50)	0.35 (0.43)
Noise	-1.96 (0.62)	0.37 (0.86)	1.70 (0.93)	-1.07 (0.72)

Relative to the reference cluster (cluster 1), characterised by those who successfully transitioned to stable employment after a short period of training, the positive ‘FMPR’ coefficients indicate that those whose father’s current or most recent job is professional or managerial are more likely to belong to clusters 3, 6, 8, and 9. These clusters are characterised by extended periods of higher education and/or further education. Conversely, clusters 2, 4, 5, and 7 have negative ‘FMPR’ coefficients. The effect is particularly pronounced for cluster 4, which mostly comprises subjects who immediately entered employment.

Those who achieved 5 or more high GCSE grades are less likely to experience joblessness (cluster 2) or to immediately enter employment (cluster 4). This suggests, as expected, that more academically inclined students tend to further their education in order to improve their job prospects. The largest positive coefficients for this covariate suggest that such students are more likely to pursue higher education after an initial 2-year period in either school (cluster 9) or further education (cluster 8). Additionally, such students are more likely to secure employment immediately after periods of further education (cluster 3) or school (cluster 7), or enter further education after prolonging their time in school (cluster 6).

Unlike the other covariates, ‘Livboth’ was not measured until June 1995. According to Figure 1, this coincides with the point by which most subjects had turned 18 and left school. Subjects who lived at home with both parents at this point are more likely to have stayed in school beyond the compulsory period and then pursued further education (cluster 6), or to have stayed in school or further education and then pursued higher education (clusters 8 and 9, respectively). Interestingly, such subjects are also more likely to belong to cluster 2, characterised by joblessness. This is the only covariate for which this is the case, perhaps suggesting that subjects who are materially supported by their parents can afford to endure extended periods of unemployment, possibly to research job opportunities in line with their expectations. Conversely, subjects who do not live at home with both parents are more likely to enter the job market sooner, either immediately (cluster 4), after long periods of training (cluster 5), or after short periods in school (cluster 7) or further education (cluster 3). However, the effects of the ‘Livboth’ coefficients appear to be slight.

The optimal $G = 10$ UCN model contains a noise component, which allows the remaining non-noise clusters to be modelled more clearly. Figure 9 focuses on this noise component, which soaks up subjects who don’t neatly fit into any of the defined clusters and transition frequently between states. This includes transitions in and out of education and in and out of employment. The only covariate with a negative coefficient associated with the noise component is ‘Livboth’. It is likely that subjects living at home are given a strong sense of direction by the influence of their parents and benefit from familial stability in terms of a lack of disruption to their parents’ marriage due to divorce or death.



Figure 9: Observations assigned to the noise component of the optimal 10-component UCN model with stepwise selection of covariates.

7 Conclusion

In [McVicar and Anyadike-Danes \(2002\)](#), Ward’s hierarchical clustering algorithm is applied to an OM dissimilarity matrix to identify relevant patterns in the data. Notably, reference is not made to the associated covariates until the uncovered clustering structure is investigated.

In particular, MLR is used to relate the assignments of the trajectories to clusters to a set of baseline covariates. It is also worth noting that the sampling weights are incorporated only in the MLR stage and not in the clustering itself. In other words, weights are incorporated only in the equivalent of the gating network. This is arguably a three-stage approach, comprising the computation of pairwise string distances using OM (or some other distance metric), the hierarchical or partition-based clustering, and the MLR.

MEDseq models, on the other hand, represent a more coherent model-based clustering approach. The sequences are modelled directly using a finite mixture of exponential-distance models, with the Hamming distance and weighted generalisations thereof employed as the distance metric. A range of precision parameter settings have been explored to allow different time points contribute differently to the overall distance. Thus, varying degrees of parsimony are accommodated. Sampling weights are accounted for by weighting each observation's contribution to the likelihood. Dependency on covariates is introduced by relating the cluster membership probabilities to covariates under the mixture of experts framework. Thus, MEDseq models treat the weights, the relation of covariates to clusters, and the clustering itself simultaneously. Model selection in the MEDseq setting identifies a reasonable solution for the MVAD data and shows that clustering the sequence trajectories in a holistic manner allows new insights to be gleaned from these data.

Opportunities for future research are varied and plentiful. Co-clustering approaches could be used to simultaneously provide clusters of the observed sequence trajectories and the time periods. While this would require the use of the CEM or stochastic EM algorithms ([Govaert and Nadif, 2013](#)), such an approach could be especially useful for the MEDseq models (CU, UU, CUN, and UUN) which weight the Hamming distance by period-specific precision parameters, as it could reduce the number of within-cluster precision parameters required to $1 < T^* \leq T$. Indeed, parsimony has been achieved in a similar fashion by [Melnykov \(2016a\)](#) in the context of finite mixtures with Markov components. In particular, co-clustering approaches which respect the ordering of the sequences by restricting the column-wise clusters to form contingent blocks may prove especially useful.

It may also be of interest for other applications to extend the MEDseq models to accommodate sequences of different lengths, for which the Hamming distance is not defined. These different lengths could be attributable to missing data, either by virtue of sequences not starting on the same date, shorter follow-up time for some subjects, or non-response for some time points. While the Hamming distance is only defined for equal-length strings, adapting the MEDseq models to such a setting would be greatly simplified if aligning the sequences of different lengths is straightforward. Another limitation of MEDseq models is that time-varying covariates are not accommodated. However, neither of these concerns are relevant for the MVAD data.

MEDseq models implicitly assume substitution-cost matrices with zero along the diagonal and a single value common to all other entries. The relationship between the exponent of an exponential-distance model based on the Hamming distance and the Hamming distance itself (which has a single substitution cost, typically equal to 1) is apparent from the fact that multiplying the substitution-cost matrix by any scalar yields the same model, because its value is absorbed into the precision parameter. This is also the case for models employing weighted Hamming distance variants under which the precision parameters, and hence the otherwise common substitution costs, vary across clusters and/or time points. However, all model types in the MEDseq family cannot account for situations in which some states are more different than others – e.g. one where the cost associated with moving from employment to joblessness is assumed to be greater than the cost associated with moving from school to training – as they assume that substitution costs are the same between each

pair of states. Such concerns are most pronounced when there is an explicit ordering to the states, e.g. education levels (Studer and Ritschard, 2016).

Hence, another potential extension is to consider MEDseq models with an alternative distance measure, particularly OM. This would require the subjective specification, or estimation, of the $v(v - 1)/2$ off-diagonal entries of symmetric substitution-cost matrices. Potentially, as per the range of precision parameter settings in the MEDseq model family, the substitution-cost matrices could also be allowed to vary across clusters and/or time points. However, the normalising constant under an exponential-distance model using OM depends both on the heterogeneous substitution costs and on θ and is not available in closed form, thereby greatly complicating model fitting. Indeed, the dependence on θ renders even offline pre-computation of the normalising constant infeasible for even moderately large T or v . Considering insertions and deletions also would present further challenges. Truncation of the sum over all sequences or an importance sampling approach could be used to address the intractability. In any case, some level of approximation would be required, while the ECM algorithm for MEDseq models based on the Hamming distance is exact.

As well as removing the normalising constant's dependence on θ , another positive consequence of the homogeneity of substitution costs with respect to pairs of states under the Hamming distance is that the ECM algorithm used for parameter estimation scales well with v , the size of the alphabet. Though restrictive, having only one parameter associated with each substitution-cost matrix, regardless of its dimensions, helps address concerns about overparameterisation, especially when the substitution costs implied by the precision parameter(s) vary across clusters and/or time points (Studer and Ritschard, 2016).

Furthermore, it is likely that results on the MVAD data would not differ greatly with OM (with state-dependent substitution costs) used in place of the Hamming distance, particularly for models where λ varies across clusters and/or time points, save for a solution with potentially fewer clusters being found. Ultimately, the weighted Hamming distance variants preserve the timing of transitions, by virtue of prohibiting insertions and deletions, but amount to improved substitution costs reflecting replacements of states.

Overall, the MEDseq models appear promising from the perspective of reconciling the distance-based and model-based cultures within the SA community. The results on the MVAD data are encouraging; they seem to suggest that the different precision parameter settings of different MEDseq models adequately address the misalignment problem inherent in the use of the Hamming distance. It remains to be seen if this holds for more turbulent sequence data, e.g. those related to employment activities tracked over longer periods.

Acknowledgements

This work was supported by the Science Foundation Ireland funded Insight Centre for Data Analytics in University College Dublin under grant number SFI/12/RC/2289_P2.

References

- Abbott, A. and J. Forrest (1986). Optimal matching methods for historical sequences. *Journal of Interdisciplinary History* 16(3), 471–494.
- Abbott, A. and A. Hrycak (1990). Measuring resemblance in sequence data: an optimal matching analysis of musician's careers. *American Journal of Sociology* 96(1), 145–185.
- Agresti, A. (2002). *Categorical Data Analysis*. New York: John Wiley & Sons.

Airoldi, E. M., D. M. Blei, E. A. Erosheva, and S. E. Fienberg (2014). *Handbook of Mixed Membership Models and Their Applications*. Chapman and Hall/CRC Press.

Banfield, J. and A. E. Raftery (1993). Model-based Gaussian and non-Gaussian clustering. *Biometrics* 49(3), 803–821.

Biernacki, C., G. Celeux, and G. Govaert (2000). Assessing a mixture model for clustering with the integrated completed likelihood. *IEEE Transactions on Pattern Analysis and Machine Intelligence* 22(7), 719–725.

Billari, F. C. (2001). The analysis of early life courses: complex description of the transition to adulthood. *Journal of Population Research* 18(2), 119–142.

Bishop, C. M. (2006). *Pattern Recognition and Machine Learning*. New York: Springer.

Böhning, D., E. Dietz, R. Schaub, P. Schlattmann, and B. G. Lindsay (1994). The distribution of the likelihood ratio for mixtures of densities from the one-parameter exponential family. *Annals of the Institute of Statistical Mathematics* 46(2), 373–388.

Bouveyron, C., G. Celeux, T. B. Murphy, and A. E. Raftery (2019). *Model-Based Clustering and Classification for Data Science: With Applications in R*. Cambridge Series in Statistical and Probabilistic Mathematics. Cambridge University Press.

Celeux, G. and G. Govaert (1992). A classification EM algorithm for clustering and two stochastic versions. *Computational Statistics and Data Analysis* 14(3), 315–332.

Celeux, G. and G. Soromenho (1996). An entropy criterion for assessing the number of clusters in a mixture model. *Journal of Classification* 13, 195–212.

Chambers, R. L. and C. J. Skinner (2003). *Analysis of Survey Data*. Chichester: John Wiley & Sons.

Dayton, C. M. and G. Macready (1988). Concomitant-variable latent-class models. *Journal of the American Statistical Association* 83(401), 173–178.

Dempster, A. P., N. M. Laird, and D. B. Rubin (1977). Maximum likelihood from incomplete data via the EM algorithm. *Journal of the Royal Statistical Society: Series B (Statistical Methodology)* 39(1), 1–38.

Gabadinho, A., G. Ritschard, N. S. Müller, and M. Studer (2011). Analyzing and visualizing state sequences in R with TraMineR. *Journal of Statistical Software* 40(4), 1–37.

Gormley, I. C. and S. Frühwirth-Schnatter (2019). Mixtures of experts models. In S. Frühwirth-Schnatter, G. Celeux, and C. P. Robert (Eds.), *Handbook of Mixture Analysis*, Chapter 12, pp. 279–316. London: Chapman and Hall/CRC Press.

Govaert, G. and M. Nadif (2013). *Co-Clustering: Models, Algorithms and Applications*. ISTE-Wiley.

Gower, J. C. (1971). A general coefficient of similarity and some of its properties. *Biometrics* 27(4), 857–871.

Hahsler, M., K. Hornik, and C. Buchta (2008). Getting things in order: an introduction to the R package seriation. *Journal of Statistical Software* 25(3), 1–34.

Hamming, R. W. (1950). Error detecting and error correcting codes. *The Bell System Technical Journal* 29(2), 147–160.

Helske, S. and J. Helske (2019). Mixture hidden Markov models for sequence data: the seqHMM package in R. *Journal of Statistical Software* 88(3), 1–32.

Helske, S., J. Helske, and M. Eerola (2016). Analysing complex life sequence data with hidden markov modeling. In G. Ritschard and M. Studer (Eds.), *Proceedings of International Conference on Sequence Analysis and Related Methods*, pp. 209–240.

Hoos, H. and T. Stützle (2004). *Stochastic Local Search: Foundations & Applications*. San Francisco, CA, USA: Morgan Kaufmann Publishers Inc.

Irurozki, E., B. Calvo, and J. A. Lozano (2019). Mallows and generalized Mallows model for matchings. *Bernoulli* 25(2), 1160–1188.

Jacobs, R. A., M. I. Jordan, S. J. Nowlan, and G. E. Hinton (1991). Adaptive mixtures of local experts. *Neural Computation* 3(1), 79–87.

Kaufman, L. and P. J. Rousseeuw (1990). Partitioning around medoids (program PAM). In *Finding Groups in Data: An Introduction to Cluster Analysis*, pp. 68–125. New York: John Wiley & Sons.

Lazarsfeld, P. F. and N. W. Henry (1968). *Latent Structure Analysis*. Boston: Houghton Mifflin.

Lesnard, L. (2010). Setting cost in optimal matching to uncover contemporaneous socio-temporal patterns. *Sociological Methods & Research* 38(3), 389–419.

Levenshtein, V. I. (1966). Binary codes capable of correcting deletions, insertions, and reversals. *Soviet Physics Doklady* 10(8), 707–710.

Linzer, D. A. and J. B. Lewis (2011). poLCA: an R package for polytomous variable latent class analysis. *Journal of Statistical Software* 42(10), 1–29.

Mallows, C. L. (1957). Non-null ranking models. *Biometrika* 44(1/2), 114–130.

McVicar, D. (2000). Status 0 four years on: young people and social exclusion in Northern Ireland. *Labour Market Bulletin* 14, 114–119.

McVicar, D. and M. Anyadike-Danes (2002). Predicting successful and unsuccessful transitions from school to work by using sequence methods. *Journal of the Royal Statistical Society: Series A (Statistics in Society)* 165(2), 317–334.

Melnykov, V. (2016a). Model-based biclustering of clickstream data. *Computational Statistics and Data Analysis* 93(C), 31–45.

Melnykov, V. (2016b). ClickClust: an R package for model-based clustering of categorical sequences. *Journal of Statistical Software* 74(9), 1–34.

Menardi, G. (2011). Density-based silhouette diagnostics for clustering methods. *Statistics and Computing* 21(3), 295–308.

Meng, X. L. and D. R. Rubin (1993). Maximum likelihood estimation via the ECM algorithm: a general framework. *Biometrika* 80(2), 267–278.

Murphy, K. and T. B. Murphy (2019). Gaussian parsimonious clustering models with covariates and a noise component. *Advances in Data Analysis and Classification*, 1–33. URL <https://doi.org/10.1007/s11634-019-00373-8>.

Murphy, K., T. B. Murphy, R. Piccarreta, and I. C. Gormley (2019). *MEDseq: mixtures of exponential-distance models with covariates*. R package version 1.0.0.

Murphy, T. B. and D. Martin (2003). Mixtures of distance-based models for ranking data. *Computational Statistics and Data Analysis* 41(3–4), 645–655.

O’Hagan, A., T. B. Murphy, L. Scrucca, and I. C. Gormley (2019). Investigation of parameter uncertainty in clustering using a Gaussian mixture model via jackknife, bootstrap and weighted likelihood bootstrap. *Computational Statistics*, 1–35. URL <https://doi.org/10.1007/s00180-019-00897-9>.

Pamminger, C. and S. Frühwirth-Schnatter (2010). Model-based clustering of categorical time series. *Bayesian Analysis* 5(2), 345–368.

Piccarreta, R. and M. Studer (2019). Holistic analysis of the life course: methodological challenges and new perspectives. *Advances in Life Course Research* 41, 100251.

R Core Team (2019). *R: a language and environment for statistical computing*. Vienna, Austria: R Foundation for Statistical Computing.

Rousseeuw, P. J. (1987). Silhouettes: a graphical aid to the interpretation and validation of cluster analysis. *Computational and Applied Mathematics* 20, 53–65.

Schwarz, G. (1978). Estimating the dimension of a model. *The Annals of Statistics* 6(2), 461–464.

Smyth, P. (2000). Model selection for probabilistic clustering using cross-validated likelihood. *Statistics and Computing* 10(1), 63–72.

Studer, M. (2013). WeightedCluster library manual: a practical guide to creating typologies of trajectories in the social sciences with R. Technical report, LIVES Working Papers 24.

Studer, M. and G. Ritschard (2016). What matters in differences between life trajectories: a comparative review of sequence dissimilarity measures. *Journal of the Royal Statistical Society: Series A (Statistics in Society)* 179(2), 481–511.

Wu, L. L. (2000). Some comments on sequence analysis and optimal matching methods in sociology: review and prospect. *Sociological Methods & Research* 29(1), 41–64.

Appendices

Appendix A The MEDseq Model Family: Parameter Counts

The models in the MEDseq family differ only in their treatments of the precision parameters, which differentiate the Hamming distance and the weighted variants thereof. While the BIC has been shown to be inadequate as a means of selecting MEDseq models, Table A.1 nevertheless summarises the number of free parameters under each MEDseq model type, in order to demonstrate the increasing level of complexity in moving from the most parsimonious CCN model to the most heavily parameterised UU model. The number of estimated parameters for each component's central sequence is treated as the sequence length T , leading to the strictest possible penalty. Note that central sequence parameters corresponding to time points with estimated or fixed precision parameter values of 0 are not counted. Note also that *estimated* precision parameter values of 0 are counted, but precision parameters fixed at 0 associated with the noise component are not counted. The number of gating network parameters is not accounted for in Table A.1; when there are gating covariates, there are $(r + 1) \times G$ extra parameters, where $r + 1$ is the dimension of the associated design matrix, including the intercept term. When mixing proportions are constrained to be equal, there are no additional parameters for models without a noise component and one additional parameter for models with a noise component; otherwise there are $G - 1$ additional parameters.

Table A.1: Number of estimated parameters under each MEDseq model type. Models with names ending with the letter N, indicating the presence of a noise component for which the single precision parameter is fixed to 0, behave like the corresponding model without this component for all other components. Thus, λ and all subscript variants thereof refer to the non-noise components only.

Model	Precision	λ_g (Clusters)	λ_t (Time Points)	Number of Parameters	
				Central Sequence(s)	Precision
CC	$\lambda_{g,t} = \lambda$	Constrained	Constrained	$GT\mathbb{1}(\lambda \neq 0)$	1
CCN				$(G - 1)T\mathbb{1}(\lambda \neq 0)$	$\mathbb{1}(G > 1)$
UC	$\lambda_{g,t} = \lambda_g$	Unconstrained	Constrained	$T \sum_{g=1}^G \mathbb{1}(\lambda_g \neq 0)$	G
UCN				$T \sum_{g=1}^{G-1} \mathbb{1}(\lambda_g \neq 0)$	$G - 1$
CU	$\lambda_{g,t} = \lambda_t$	Constrained	Unconstrained	$G \sum_{t=1}^T \mathbb{1}(\lambda_t \neq 0)$	T
CUN				$(G - 1) \sum_{t=1}^T \mathbb{1}(\lambda_t \neq 0)$	$\mathbb{1}(G > 1)T$
UU	$\lambda_{g,t} = \lambda_{g,t}$	Unconstrained	Unconstrained	$\sum_{g=1}^G \sum_{t=1}^T \mathbb{1}(\lambda_{g,t} \neq 0)$	GT
UUN				$\sum_{g=1}^{G-1} \sum_{t=1}^T \mathbb{1}(\lambda_{g,t} \neq 0)$	$(G - 1)T$

Appendix B Further Details on Estimating MEDseq Models

Weighted complete data likelihood functions for all model types in the MEDseq family are given in Table B.1. Table B.2 outlines the corresponding CM-steps for the precision parameter(s). The sampling weights are accounted for in all cases. The CM-step formulas can be simplified somewhat for unweighted models. Recall that the first letter of the model name denotes whether the precision parameters are constrained/unconstrained across clusters, the second denotes the same across time points (i.e. sequence positions), and model names ending with the letter N include a noise component. All models are written as though gating network covariates \mathbf{x}_i are included. Moreover, models with a noise component are written in the GN rather than NGN form, i.e. it assumed that the covariates affect the mixing proportions of the noise component rather than τ_0 being constant (see Section 4.1). All derivations closely follow the same steps as in Section 4.1.3 for the CC model.

Table B.1: Weighted complete data likelihood functions for all MEDseq model types, which differ according to the constraints imposed on the precision parameters across clusters and/or time points. The expressions for the various weighted Hamming distance metric variants employed are given in full.

Model	Weighted Complete Data Likelihood
CC	$\prod_{i=1}^n \left[\prod_{g=1}^G \left(\tau_g(\mathbf{x}_i) \frac{\exp(-\lambda \sum_{t=1}^T \mathbb{1}(s_{i,t} \neq \theta_{g,t}))}{((v-1)e^{-\lambda} + 1)^T} \right)^{z_{i,g}} \right]^{w_i}$
UC	$\prod_{i=1}^n \left[\prod_{g=1}^G \left(\tau_g(\mathbf{x}_i) \frac{\exp(-\lambda_g \sum_{t=1}^T \mathbb{1}(s_{i,t} \neq \theta_{g,t}))}{((v-1)e^{-\lambda_g} + 1)^T} \right)^{z_{i,g}} \right]^{w_i}$
CU	$\prod_{i=1}^n \left[\prod_{g=1}^G \left(\tau_g(\mathbf{x}_i) \frac{\exp(-\sum_{t=1}^T \lambda_t \mathbb{1}(s_{i,t} \neq \theta_{g,t}))}{\prod_{t=1}^T ((v-1)e^{-\lambda_t} + 1)} \right)^{z_{i,g}} \right]^{w_i}$
UU	$\prod_{i=1}^n \left[\prod_{g=1}^G \left(\tau_g(\mathbf{x}_i) \frac{\exp(-\sum_{t=1}^T \lambda_{gt} \mathbb{1}(s_{i,t} \neq \theta_{g,t}))}{\prod_{t=1}^T ((v-1)e^{-\lambda_{gt}} + 1)} \right)^{z_{i,g}} \right]^{w_i}$
CCN	$\prod_{i=1}^n \left[\prod_{g=1}^{G-1} \left(\tau_g(\mathbf{x}_i) \frac{\exp(-\lambda \sum_{t=1}^T \mathbb{1}(s_{i,t} \neq \theta_{g,t}))}{((v-1)e^{-\lambda} + 1)^T} \right)^{z_{i,g}} \left(\frac{\tau_0(\mathbf{x}_i)}{v^T} \right)^{z_{i,0}} \right]^{w_i}$
UCN	$\prod_{i=1}^n \left[\prod_{g=1}^{G-1} \left(\tau_g(\mathbf{x}_i) \frac{\exp(-\lambda_g \sum_{t=1}^T \mathbb{1}(s_{i,t} \neq \theta_{g,t}))}{((v-1)e^{-\lambda_g} + 1)^T} \right)^{z_{i,g}} \left(\frac{\tau_0(\mathbf{x}_i)}{v^T} \right)^{z_{i,0}} \right]^{w_i}$
CUN	$\prod_{i=1}^n \left[\prod_{g=1}^{G-1} \left(\tau_g(\mathbf{x}_i) \frac{\exp(-\sum_{t=1}^T \lambda_t \mathbb{1}(s_{i,t} \neq \theta_{g,t}))}{\prod_{t=1}^T ((v-1)e^{-\lambda_t} + 1)} \right)^{z_{i,g}} \left(\frac{\tau_0(\mathbf{x}_i)}{v^T} \right)^{z_{i,0}} \right]^{w_i}$
UUN	$\prod_{i=1}^n \left[\prod_{g=1}^{G-1} \left(\tau_g(\mathbf{x}_i) \frac{\exp(-\sum_{t=1}^T \lambda_{gt} \mathbb{1}(s_{i,t} \neq \theta_{g,t}))}{\prod_{t=1}^T ((v-1)e^{-\lambda_{gt}} + 1)} \right)^{z_{i,g}} \left(\frac{\tau_0(\mathbf{x}_i)}{v^T} \right)^{z_{i,0}} \right]^{w_i}$

Table B.2: CM-steps for the precision parameter(s) for all MEDseq model types, which differ according to the constraints imposed across clusters and/or time points.

Model	Precision Parameter CM-steps
CC	$\hat{\lambda}^{(m+1)} = \max \left(0, \log(v-1) + \log \left(\frac{T \sum_{i=1}^n \sum_{g=1}^G \hat{z}_{i,g}^{(m+1)} w_i}{\sum_{i=1}^n \sum_{g=1}^G \hat{z}_{i,g}^{(m+1)} w_i d_H(\mathbf{s}_i, \hat{\theta}_g^{(m+1)})} - 1 \right) \right)$
UC	$\hat{\lambda}_g^{(m+1)} = \max \left(0, \log(v-1) + \log \left(\frac{T \sum_{i=1}^n \hat{z}_{i,g}^{(m+1)} w_i}{\sum_{i=1}^n \hat{z}_{i,g}^{(m+1)} w_i d_H(\mathbf{s}_i, \hat{\theta}_g^{(m+1)})} - 1 \right) \right)$
CU	$\hat{\lambda}_t^{(m+1)} = \max \left(0, \log(v-1) + \log \left(\frac{\sum_{i=1}^n \sum_{g=1}^G \hat{z}_{i,g}^{(m+1)} w_i}{\sum_{i=1}^n \sum_{g=1}^G \hat{z}_{i,g}^{(m+1)} w_i \mathbb{1}(s_{i,t} \neq \hat{\theta}_{g,t}^{(m+1)})} - 1 \right) \right)$
UU	$\hat{\lambda}_{g,t}^{(m+1)} = \max \left(0, \log(v-1) + \log \left(\frac{\sum_{i=1}^n \hat{z}_{i,g}^{(m+1)} w_i}{\sum_{i=1}^n \hat{z}_{i,g}^{(m+1)} w_i \mathbb{1}(s_{i,t} \neq \hat{\theta}_{g,t}^{(m+1)})} - 1 \right) \right)$
CCN	$\hat{\lambda}^{(m+1)} = \max \left(0, \log(v-1) + \log \left(\frac{T \sum_{i=1}^n \sum_{g=1}^{G-1} \hat{z}_{i,g}^{(m+1)} w_i}{\sum_{i=1}^n \sum_{g=1}^{G-1} \hat{z}_{i,g}^{(m+1)} w_i d_H(\mathbf{s}_i, \hat{\theta}_g^{(m+1)})} - 1 \right) \right)$
UCN	$\hat{\lambda}_g^{(m+1)} = \max \left(0, \log(v-1) + \log \left(\frac{T \sum_{i=1}^n \hat{z}_{i,g}^{(m+1)} w_i}{\sum_{i=1}^n \hat{z}_{i,g}^{(m+1)} w_i d_H(\mathbf{s}_i, \hat{\theta}_g^{(m+1)})} - 1 \right) \right)$
CUN	$\hat{\lambda}_t^{(m+1)} = \max \left(0, \log(v-1) + \log \left(\frac{\sum_{i=1}^n \sum_{g=1}^{G-1} \hat{z}_{i,g}^{(m+1)} w_i}{\sum_{i=1}^n \sum_{g=1}^{G-1} \hat{z}_{i,g}^{(m+1)} w_i \mathbb{1}(s_{i,t} \neq \hat{\theta}_{g,t}^{(m+1)})} - 1 \right) \right)$
UUN	$\hat{\lambda}_{g,t}^{(m+1)} = \max \left(0, \log(v-1) + \log \left(\frac{\sum_{i=1}^n \hat{z}_{i,g}^{(m+1)} w_i}{\sum_{i=1}^n \hat{z}_{i,g}^{(m+1)} w_i \mathbb{1}(s_{i,t} \neq \hat{\theta}_{g,t}^{(m+1)})} - 1 \right) \right)$

Appendix C MVAD Data: Gating Network Coefficients

Multinomial logistic regression coefficients and associated WLBS standard errors for the gating network of a $G = 10$ UCN model with stepwise selection of covariates are provided in Table 6. For completeness, coefficients and WLBS standard errors for an otherwise equivalent model with all covariates included (except those used to define the sampling weights) are given in Table C.1. Such a model achieves a wDBS value of 0.4717 (see Table 3), compared to 0.4745 for the optimal model with only a subset of covariates detailed in Section 5.1. Notably, $G = 10$ and the UCN model type are both also optimal according to the wDBS criterion for the model with all covariates included.

Table C.1: Multinomial logistic regression coefficients and associated WLBS standard errors (in parentheses) for the gating network of the 10-component UCN model with all covariates included.

Cluster	(Intercept)	Gender	Catholic	Funemp	GCSE5eq	FMPR	Livboth
2	-1.29 (0.68)	-0.57 (0.54)	1.10 (0.69)	1.50 (0.59)	-0.06 (0.68)	0.36 (0.65)	-0.04 (0.53)
3	0.10 (0.49)	-0.55 (0.39)	0.21 (0.40)	0.50 (0.54)	1.25 (0.49)	0.50 (0.47)	-0.27 (0.38)
4	0.66 (0.50)	-0.19 (0.39)	-0.23 (0.39)	-0.09 (0.51)	-0.29 (0.51)	-0.86 (0.42)	-0.16 (0.39)
5	-1.16 (0.57)	1.24 (0.49)	0.39 (0.42)	-0.17 (0.59)	0.24 (0.61)	-0.26 (0.56)	-0.14 (0.44)
6	-2.52 (1.09)	-0.57 (0.61)	0.65 (0.70)	0.41 (1.10)	1.97 (0.77)	0.83 (0.70)	1.46 (0.74)
7	0.10 (0.63)	-0.76 (0.54)	-0.05 (0.53)	0.26 (0.72)	1.32 (0.59)	-0.50 (0.63)	0.03 (0.53)
8	-2.86 (0.63)	-0.60 (0.46)	-0.04 (0.47)	-0.24 (0.71)	3.24 (0.55)	0.31 (0.54)	1.17 (0.48)
9	-1.82 (0.63)	-0.40 (0.42)	0.58 (0.43)	-0.35 (0.70)	3.77 (0.53)	0.82 (0.48)	0.41 (0.46)
Noise	-1.76 (0.67)	0.40 (1.02)	-0.93 (0.97)	0.48 (0.85)	1.34 (0.99)	0.03 (0.98)	-0.65 (0.86)